



People's Democratic Republic of Algeria
Ministry of Higher Education and Scientific Research
University of Kasdi Merbah Ouargla

Faculty of Hydrocarbons, Renewable Energies, Earth and Universe Sciences.

Department of Renewable Energies.

ACADEMIC MASTER THESIS

Filiere: Mechanical Engineering.

Domain: Renewable Energy

Specialty: Renewable Energy in Mechanics.

Presented by:

Ikram LAGGOUN

Romaissa DJABOREBBI

Theme:

**CFD simulation for enhancing heating room efficiency
using a trombe wall.**

Publicly defended on :06/06/2024

Before the jury:

Dr. Med El-Hafed Berbeh	MCB Professor (UKM Ouargla)	Charman
Dr. Zineb Chaich	MCB Professor (UKM Ouargla)	Examiner
Dr. Djamel Belatrache	MCB Professor (UKM Ouargla)	Supervisor

Academic year: 2023/2024

اهداء

قال تعالى: (يَرْفَعِ اللَّهُ الَّذِينَ آمَنُوا مِنْكُمْ وَالَّذِينَ أُوتُوا الْعِلْمَ دَرَجَاتٍ) (المجادلة 11)

ويقول النبي ﷺ في الحديث الصحيح من (سلك طريقا يلتمس به علما؛ سهل الله به طريقا إلى الجنة)

بعد الحمد لله الذي هدانا الى علم ننتفع به لا يسعني بعد سنوات طوال من الكد والاجتهاد والتضحية الا ان اشكر شخصي المفضل داعمي الأول فما انا الا به الى ابي ادمك الله كل الشكر والحب الى من ساهم في نجاحي الى عائلتي الى امي واخوتي كل باسمه. شكرا لزملاء الدراسة ولكل اسرة الطاقات المتجددة من أساتذة الى موظفين القسم.

إكرام

اهداء

هذا اليوم ليس نهاية المطاف بل هو خطوة نحو تحقيق الأهداف وتحقيق الطموحات.

بالتخرج اليوم نثبت اننا قادرين على تجاوز التحديات وتحقيق الانجازات

اهدي هذا العمل المتواضع.

لمن كانا سببا في وجودي وسندي على اكمال دراستي "ابي و امي" الى زهراتي اخواتي

وقرة عيني اخوتي الى 'جدتي' الغالية اطل الله في عمرها

كما لا أنسى أصدقائي وافراد عائلتي ولكل من اعطاني يد العون من قريب او بعيد.

والى كل اسرة قسم الطاقات المتجددة.

رميضاء

شكر وتقدير

ولا يسعنا إلا أن نشكر كل من ساهم بشكل مباشر أو غير مباشر

في إنجاز هذا العمل، وعلى وجه الخصوص الأستاذ المشرف بالأطرش جمال

وأساتذة قسم الطاقات المتجددة في الميكانيك الذين كان لهم الفضل في

وصولنا الى هذا النجاح: بوشكيمة بشير، بريح م الحافظ، شايش زينب، رواق عمر،

معمور حسين، حجاج. ع السميع، حجاج. ع الصادق، بلوفي يوسف، دواق. عماري

شعيب, العناني، بن منين جمال، دبي. ع م، غربي أبراهيم

ولا ننسى جهود الانسة اسمهان على مسانبتها واعانتها لنا

وشكر خاص لزملاء الدراسة

Content

اهداء.....	II
شكر وتقدير.....	III
CONTENT	IV
LISTE OF FIGURES	VI
LISTE OF TABLES	VII
NOMENCLATURE.....	VIII
GENERAL INTRODUCTION	1

CHAPTER I

AN UPDATE ON RENEWABLE ENERGIES HEATING SYSTEM

I.1 INTRODUCTION.....	3
I.2 Renewable Energy Sources	3
I.3 Heating system	3
I.4 Types of Heating Renewable	4
I.4.1 Solar heating.....	4
I.4.1.1 Passive solar heating systems.....	4
I.4.1.2 Active solar systems.....	6
I.4.2 Geothermal energy	7
I. 4.2.1 Ground water heat pump (GSHP)	8
I.4.2.2 Surface water heat pumps	8
I. 4.2.3 Ground coupled heat pumps.....	9
I.4.3 Biomass energy heating	9
I.4.4 Green Hydrogen	10
I.5 A overview of some renewable heating projects	11
I.6 Conclusion.....	21

CHAPTER II

MATHEMATICAL MODELING OF A HEATING SYSTEM FOR A LIVING ROOM

II.1 INTRODUCTION	23
II.2 Presentation of the study region.....	23
II.3 Climate data	24

II.3.1 Solar radiation (w/m ²) for the Ouargla region 2023-2019.....	24
II.3.2 Temperature (C°) Data for the Ouargla region 2023-2019.....	24
II.3.3 Wind Speed data (km/h) for Ouargla region 2023 -2019	25
II.3.4 Humidity (%) data for Ouargla region 2023-2019.	25
II.4 Modeling the thermal behavior of building component	26
II.5 Modeling the thermal behavior of a building	27
II.5.1 Model of a wall without insulation	27
II.5.2 Model of a window without insulation	27
II.5.3 Model of a door without insulation.....	27
II.5.4 Model of a ceiling without insulation	27
II.5.5 Model of a heated floor.....	27
II.6 Room ambient temperature model.....	28
II.7 GOVERNING EQUATIONS IN 2D.....	28
II.8 BOUNDARY CONDITIONS	28
II.9 Conclusion:	29

CHAPTER III
SIMULATION RESULTS.

III.1 INTRODUCTION.....	31
III.2 Grid size test	33
III.3 Solution control (convergence)	34
III.4 VALIDATION OF RESULTS	35
III.5 RESULTS AND DISCUSSIONS	35
III.5.1 Top outlet.....	36
III.5.2 Middle outlet.....	38
III.6 Conclusion	42
GENERAL CONCLUSION.....	44
ABSTRACT	45
BIBLIOGRAPHY	48

Liste of Figures

Figure I-1: Overview of renewable energy sources.....	3
Figure I- 2: Direct solar gains in building	4
Figure I-3: Desing of Trombe wall.....	5
Figure I-4: isolated gains in building.....	6
Figure I-5: Geothermal energy pumps for heating and cooling purposes.	7
Figure I-6: Biomass conversion process.....	10
Figure I-7: A solar thermal system of DHW pro du space heating and cooling.	12
Figure I-8: Schematic of an Aquifer Thermal Energy Storage (ATES).....	13
Figure I-9: Multi-faceted geothermal system	14
Figure I-10: Depicting heat transfer from deep geothermal system.....	14
Figure I-11: Schematic of a novel domestic heating system.	15
Figure I-12: A graphical illustration of the proposed smart building energy system driven by renewable sources	15
Figure I-13: Physical model of solar chimney.....	18
Figure I -14: Wind Towers.	19
Figure I -15: The sketch of the simulated refrigeration cabinet.....	20
Figure I-16: physical model for winter heating system in 2D.....	20
Figure II-1: Wilaya of Ouargla, Algeria.	23
Figure II- 2: Solar radiation data	24
Figure II-3: Temperature (C°) Data.....	25
Figure II- 4: Wind speed data	25
Figure II-5: Humidity data.....	26
Figure III -1: Physical model for heating system in 2D.	31
Figure III-2: Grid size test.	34
Figure III-3: Convergence Curve.	35
Figure III-4: Contours of static temperature (C°) [TOP Outlet 0.01].....	36
Figure III-5: Contours of static Velocity (m/s) [TOP Outlet0.01].	37
Figure III-6: Velocity change curve as a function of distance.	37
Figure III-7: Contours of static temperature (C°) [middle Outlet0.01].	38
Figure III-8: Contours of static velocity (m/s) [middle Outlet0.01].....	39
Figure III-9: Velocity change curve as a function of distance	39
Figure III-10: Contours of static temperate (C°) [Bottom Outlet0.01]	40

Figure III-11: Contours of static Velocity (m/s) [Bottom Outlet 0.01].	41
Figure III-12: Velocity change curve as a function of distance.	41

Liste of Tables

Table I-1: Hydrogen color shades and their Technology, cost, and CO2 emissions	11
Table II-1: Characteristics of building elements	26
Table III-1: Trombe Wall model dimensions	31
Table III -2: Settings and model in fluent program	32
Table III-3: Zones type and continuum Condition in fluent program	32
Table III-4: Zones type and boundary condition	32
Table III-5: Factors in fluent program	33
Table III-6: Mesh size used in our work	33
Table III-7: The residuals for the governing equations	34

Nomenclature

AC :	Ceiling Surface (m ²)
ACH :	Air Coupled Heating
AF :	Floor Area (m ²)
AG :	Window Area (m ²)
AWE :	Wall Area (East) (m ²)
AW :	Wall Surface (m ²)
AWN :	Wall Surface (North) (m ²)
AWS :	Wall Surface (South) (m ²)
AWOE :	Wall Surface (West) (m ²)
AD :	1 When the Door is Open
AD :	0 When the Door is Closed
CA :	Thermal Capacity of Air (J/K)
CW :	Thermal Capacity of The Wall (J/K)
CSD :	Solar Thermal Capacity of The Door (J/K),
CC :	Thermal Capacity of The Ceiling (J/K)
CP :	Power Coefficient
DHC :	District Heating and Cooling
ETC :	Evacuated Tube Collectors
FPC :	Flat-Plate Collectors
GHX :	Ground Heat Exchangers

GWP : Groundwater Heat Pump

GWHPs : Groundwater Heat Pump Systems

GCHPS : Ground-Coupled Heat Pump Systems

HVAC : Heating Vertical Alternative to Consider

HEP : High Energy Performance

HIL : Hardware-In-the-Loop

INA : National Institute of Agriculture

m : mass flow of the expensive jet (kg s)

M : the mass of the fluid (Kg)

m^ob-out : the output mass flow (Kg s)

m^ob-in : the input mass iuX (Kgs)

Op : specific heat capacity J/kgk)

P : window factor

Qe : thermal flow of interior equipment (W)

Qg-air : thermal flow of the window (W)

Qs : solar thermal ux (W)

QWATER : Thermal Flow of Water (W) Which Constitutes the Heat Supply

SEE : thermal capacity of the floor (J/K)

SWHPs : Surface Water Heat Pump Systems

TAI : Indoor Air Temperature (°C)

TAO : Outdoor Air Temperature (°C)

TAIA : Indoor Air Temperature of Room A (°C)

TAIB : Indoor Air Temperature of Room B (°C)

TC : Ceiling Temperature (°C)

TD : Door Temperature (°C)

Tf :	Floor Temperature (°C)
Tw :	Wall Temperature (°C)
Tw _e :	Wall Temperature (east) (°C)
Tw _s :	Wall Temperature (north) (°C)
Tw _s :	Wall Temperature (south) (°C)
Tb-out :	The Temperature at the Outlet of the Fluid (C)
TB-IN :	The Temperature of the Inlet Fluid (C)
TF-IN :	Indoor Floor Temperature (C)
TF-OUT :	Outside Floor Temperature (°C)
TWOE :	Wall Temperature (west) (°C)
UWI :	interior thermal transfer coefficient of the wall (W/m ² K)
UWO :	external thermal transfer coefficient of the wall (W/m ² K)
UD :	thermal transfer coefficient of the door (W/m ² K)
UCI :	interior thermal transfer coefficient of the ceiling (W/m ² K)
UCO :	external thermal transfer coefficient of the ceiling (W/m ² K)
UF :	thermal transfer coefficient of the floor (W/m ² K),
UWIS :	interior thermal transfer coefficient of the wall (north) (W/m ² K)
UWIN :	interior thermal transfer coefficient of the wall (north) (W/m ² K)
UWIE :	interior thermal transfer coefficient of the wall (east) (W/m ² K)
UWIOE :	interior heat transfer coefficient of the wall (west) (W/m ² K)
VGHX :	Vertical Ground Heat Exchangers
λ :	the tip speed ratio

General introduction

General introduction

Solar energy could one day replace fossil energy in all areas. After studies proved that solar energy succeeded in producing continuous renewable electricity throughout the day and after solar drying was able to be one of the methods that contribute significantly to the manufacture of dried fruits and vegetables in a food-safe manner. In the shortest possible time, solar thermal energy has almost succeeded in heating water for our daily use. Because heating requires high energy, and because traditional heating methods rely on fossil energy, they have become ineffective because they negatively affect the environment and cause the release of carbon dioxide gas in large quantities. Also, due to the large population and increased demand for energy, we have fallen into an energy crisis. For this reason, the world's resort to renewable sources is the most rational alternative, in addition to being harmless to the environment. Trombe wall is a kind of passive solar. It is an external glass surface placed in front of a concrete wall to create a greenhouse effect to warm the air between them. The air passes into the house through two openings in the wall an upper opening to enter hot air and a lower opening to expel cold air. Therefore, the Trombe wall only needs the well-known physical phenomenon, which is convection.

This research aims to verify the feasibility of using the trombe wall as a ventilation and heating system in the living room , and arriving at a design that gives us the best performance of the trombe wall to warm the room in some way. This thesis has been divided into three chapters:

The first chapter dealt with generalities in renewable heating and its types, explained them, and also provided an overview of renewable heating projects and how they work.

The second chapter shed light on understanding and modeling thermal behavior in buildings, where heat transfer equations were developed for building elements (wall, ceiling, floor, etc.) without insulation, and then it dealt with modeling thermal storage of building elements for the living room.

As for the third and final chapter of the study, we discussed the effect of adding a trombe wall system on the air temperature and velocity distribution within the living area of the room and the effect of the outlet location on heat transfer using the GAMBIT and Fluent programs.

Finally, the research ends with a general result that explains the effect of the Trombe wall on the living room.

Chapter I

An update on renewable energies heating system

I.1 Introduction

This chapter presents definitions, types, and latest updates for renewable energy heating systems (Figure I-1). This innovation promises efficient and environmentally friendly heating solutions. With advances in technology, these systems have become more accessible and cost-effective. This represents an important step towards reducing our carbon footprint and promoting a greener future. Renewable energies are defined as those energies that are generated naturally and sustainably; it is not depleted and is available in nature in an unlimited and sometimes limited manner, but it is constantly renewed, in addition to being clean and its use does not result in any environmental pollution.

I.2 Renewable Energy Sources

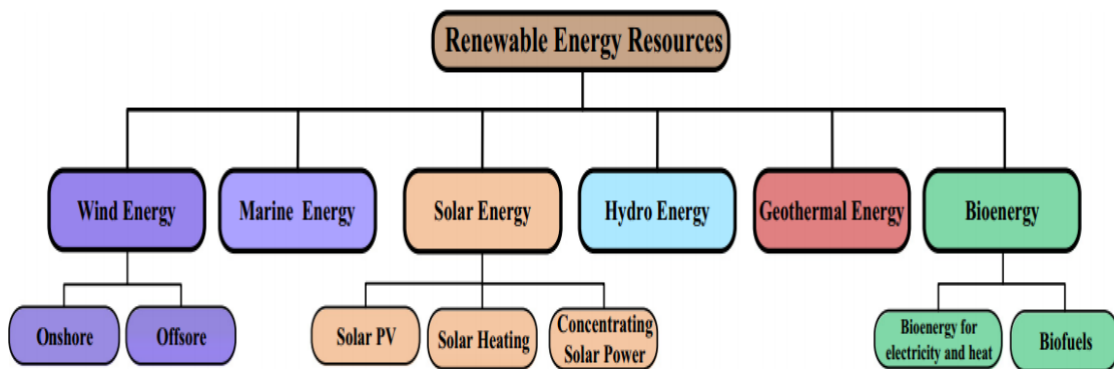


Figure I-1: Overview of renewable energy sources. [1]

I.3 Heating system

A heating system is a mechanism used to generate and distribute heat within a building or space to maintain a comfortable temperature. There are different types of heating systems available as represented in figure I01, each with their own advantages and applications

a. Direct heating: in which the heat generator is placed inside the place to be heated. It is used to heat only one place.

b. Indirect heating: or central heating: in which one thermal generator is used to heat several places, and this generator is placed outside the places to be heated.

It heats the heat transfer medium (water, air, steam) supply network and the pipes are called the return network and are marked with a dashed line.[2]

I.4 Types of Heating Renewable

I.4.1 Solar heating

Choosing the right HVAC system for the home can bring us benefits in terms of well-being and economic savings. Solar heating is an alternative to consider, as it reduces the environmental impact of heating or cooling a home solar heating system can be divided into two main types, the first is called a passive solar heating systems and the other is called active solar heating systems.

I.4.1.1 Passive solar heating systems

The aspects related to solar energy, namely collection storage and distribution, are carried out in natural ways, and no form of mechanical or electrical energy or other electronic control devices is used [3]. There are three basic types of passive solar design: direct gain, indirect gain, and isolated gain. The purpose of all of them is the passive solar space heating, which can contribute to the significantly reducing of building energy consumption.

a) Direct gains

Direct gain is the simplest passive design technique (Figure I-2). Sunlight enters the house through the aperture - usually south-facing windows with a glazing material made of transparent or translucent glass, and virtually all of solar energy can be converted into thermal energy. The sunlight then strikes masonry floors and/or walls, which absorb and store the solar heat. The surfaces of these masonry floors and walls are typically a dark color because dark colors usually absorb more heat than light colors [4].

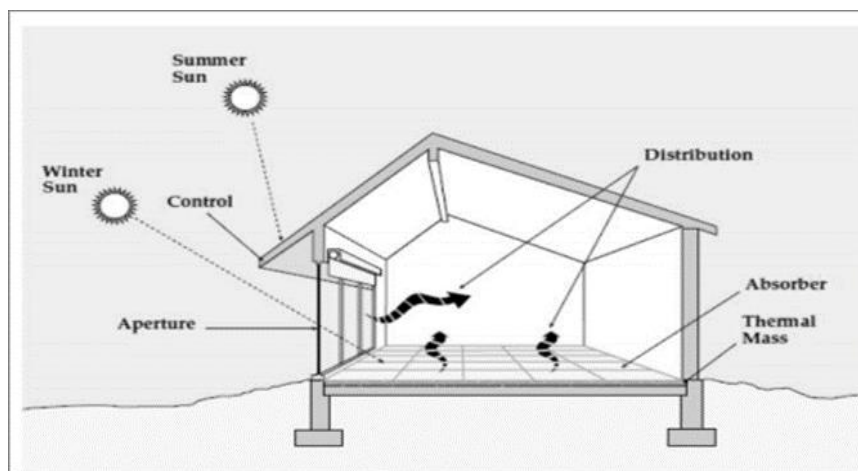


Figure I- 2: Direct solar gains in building [4]

b) Indirect gains

An indirect gain system uses the basic elements of heat collection and storage in combination with convection. In this approach, Trombe wall is the most common indirect-gain approach, when a dark-colored thermal storage wall is placed behind a south-facing window and in front of the living space. The Trombe wall (figure I-3) consists of thick masonry wall on the south side of a house. A single or double layer of glass is mounted about 1 inch or less in front of the wall's surface. Heated air flows out through heat-distributing vents at the top of the wall while vents at the bottom of the wall draw in cool air into the heating space. The top and bottom vents continue to circulate air as long as the air entering the bottom vent is cooler than the air leaving the top vent. Consequently, the storage mass continues to heat the interior space by radiation for six to eight hours. As the mass warms and then gives off heat, it keeps temperatures in the living space fairly uniform. It also means that the heating of the living area occurs in the evening and at night.[4]

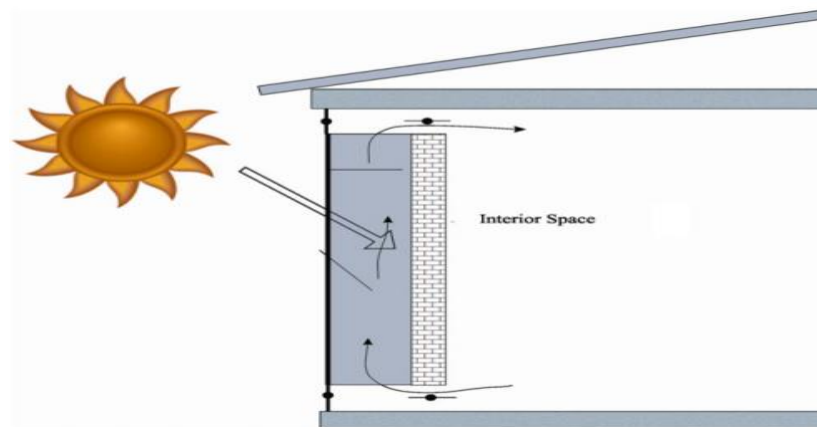


Figure I-3: Design of Trombe wall [5]

c) Isolated gains

A sunspace - also known as a solar room or solarium is a versatile approach to passive solar heating. It can project from the house or be partially enclosed within the house. Typically, the sunspace is a separate room on the south side of the house with a large glass area and thermal storage mass as shown in (Figure I-4). A sunspace can be built as part of a new home or as an addition to an existing one. The simplest and most reliable sunspace design is to install vertical windows with no overhead glazing. Sunspaces may experience high heat gain and high heat loss through their abundance of glazing; the temperature variations caused by the heat losses and gains can be moderated by thermal mass and low-emissivity windows. The thermal mass that can be used includes a masonry floor, a masonry

wall bordering the house, or water containers. The distribution of heat to the house can be accomplished through ceiling and floor level vents, windows, doors, or fans. Most homeowners and builders also separate the sunspace from the home with doors and/or windows so that home comfort isn't overly affected by the sunspace's temperature variations. Sunspaces may often be called and look a lot like "greenhouses". [4]

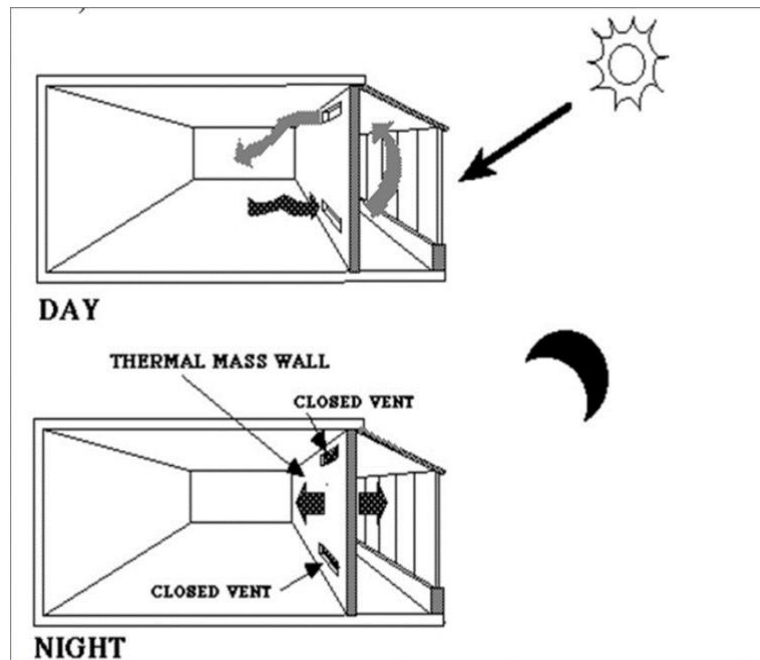


Figure I-4: isolated gains in building [6]

I.4.1.2 Active solar systems

a. Solar collectors: A solar collector is a heating device that harnesses the solar energy and converts it to useful heat which is transferred to the heating fluid circulating through the collector.[7]

b. Flat-plate collectors (FPC): A flat panel collector (FPC) it is commonly used to collect solar thermal energy at low ambient temperatures. It consists of a selectively coated absorption plate, a heating fluid to extract heat from the absorption plate, tubes for the flow of the heating fluid, a transparent cover to increase the greenhouse effect and reduce overhead heat loss, a heat-insulating backing to reduce heat loss and a protective sleeve to ensure that the components are free from moisture and dust. Some disadvantages of this configuration were irregular temperature distribution on the absorption surface and increased heat loss resulting from increased temperature under low flow rate conditions. Therefore, serpentine tube design was introduced to overcome these problems. It is designed primarily to compensate for low flow rate conditions; The design allows the mass flow rate to be regulated through the tube,

increasing the heat transfer coefficient. The core component of FPC is the absorber, and its thermal performance depends on the design parameters as well as material properties .[7]

c. Evacuated tube collectors: Evacuated tube collectors (ETC) have been commercially available for more than 20 years, ETC consists of: evacuated tubes (glass-glass seal) to minimize heat losses, copper heat pipes for rapid heat transfer, and aluminum casing to provide durability and structural integrity to the system. ETC minimizes the heat losses due to convection and radiation. [8]

I.4.2 Geothermal energy

The noun geothermal can be divided into two words: geo, which means earth, and thermal, which means heat. The soil is a stable temperature at an approximate 6–10 m in the range of 16–29°C all year round; it can be exploited for energy generation, cooling and heating buildings, or using direct underground heat [9]. There are many advantages to geothermal energy potentials that must not be taken for granted. In general, exploiting geothermal energy falls into two categories, which are:

- Heating in cold seasons: since the temperature in the ground is higher than the atmosphere's temperature, sometimes it is sufficient for heating or only preheating. Moreover, applying and taking advantage of heat pumps highly increases heat removal from the ground (figureI-5).
- Cooling in hot seasons: underground temperature is cooler than temperature above the ground and the difference enables good use of it for cooling or precooling (Figure I-5). Again, heat pumps used in reverse mode (cooling mode) can enhance the efficiency and the temperature provided for cooling can be lowered. [10]

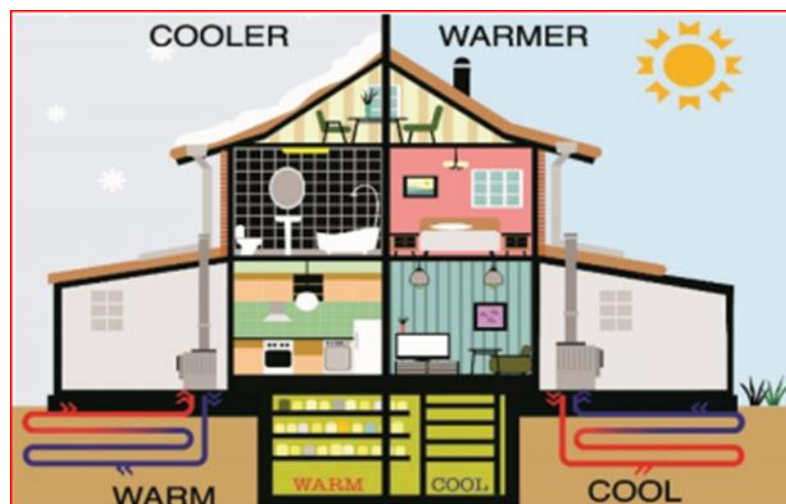


Figure I-5: Geothermal energy pumps for heating and cooling purposes. [11]

Geothermal heat pumps are a renewable energy technology for heating and cooling. These systems combine heat pumps and geothermal fields and use groundwater or surface water as a source of heat these systems combine heat pumps and geothermal fields. Geothermal heat pumps can be divided into three main types, depending on the type of external heat exchange system geothermal heat pump systems (GWP):

- Groundwater heat pump systems (GWHPs).
- Surface water heat pump systems (SWHPs).
- Ground-coupled heat pump systems (GCHPs).

I. 4.2.1 Ground water heat pump (GSHP)

All heat pumps work between a high and low temperature. The low temperature medium is called a heat source (TL) and the high temperature medium is called a heat sink (TH). A ground-source heat pump or geothermal heat pump has the ground as its heat source or sink.

Here, GHE plays a role exchanging heat between the ground and the heat pump. Moreover, a heating or cooling coil is tasked with exchanging heat between the heat pump and a space. Sinks and sources of heat pumps are different in heating and cooling seasons. When cooling (inserting heat into the ground), heat is exchanged from a cooling coil (low-temperature medium) to a refrigerant flowing in the GHE (high-temperature medium). However, in heating seasons (heat removal from the ground), heat is exchanged with a refrigerant flowing in the GHE (low-temperature medium) to a heating coil (high-temperature medium). [10]

I.4.2.2 Surface water heat pumps

These heat pumps use the surface water as heat source or sink. In general, the surface water bodies have ideal thermal characteristics as heat source. The temperature profile over the year including the maximum and the minimum temperatures of the water body, which is in direct contact with the atmosphere, are very suitable for efficient operation of the heat pump, especially in cooling mode. the SWHPs can be either closed-loop systems or open-loop systems as the following:

- **The closed-loop system:** the closed-loop SWHPs is similar to GCHPs. It consists of water-to-water or water-to-air heat pumps linked to a submerged piping loop (coils) that transfers heat to or from the water pump when transfers heat to or from the air in the building and then exchanges it to or from the lake by the working fluid circulating inside the submerged coil.

- **The open-loop system:** the open-loop SWHPs is similar to GWHPs. In these systems, the water-to-water or water-to-air heat pump unit pumps water from water body through a heat exchanger and then returns it to the lake some distance from the point in which it was removed. The water can be pumped directly to the heat pumps unit or to an intermediate heat exchanger that is connected to the unit with a closed piping loop. [12]

I. 4.2.3 Ground coupled heat pumps

The ground coupled heat pumps also called closed loop ground source heat pumps, consists of a reversible heat pump that is linked to a closed loop, i.e. ground heat exchanger. In these systems, the heat is extracted from or rejected to the ground via buried pipes, through which pure water or antifreeze fluid circulates. the (GCHPs) are categorized according to ground heat exchanger types that include horizontal ground heat exchangers and vertical ground heat exchangers (VGHX). The horizontal (GHX): the (HGHX) means the heat exchangers that installed horizontally at a few meter below the ground surface. As with all the (GHX) types, the horizontal ground heat exchanger consists of (HDPE) (high-density polyethylene) pipes through which heat exchange fluid are circulated. it can be divided into three subgroups: linear, slinky and spiral coil-type ,the vertical (GHX): the u-tube heat exchangers installed vertically in the ground are called vertical ground heat exchangers. These types of heat exchangers have many configurations ,which can be installed in a one, tens, or even hundreds of boreholes according to the thermal loads. The design of vertical ground heat exchangers is complicated by many constraints that include the variety of geological formation at the installation site as well as the huge initial investment cost especially with the large projects. [12]

I.4.3 Biomass energy heating

Biomass is an alternative energy to fossil fuels. Converting biomass into usable fuel requires transformation processes for their energy exploitation. Two procedures for biomass transformation (Figure I-6): -Biochemical process -Thermochemical process. [13]

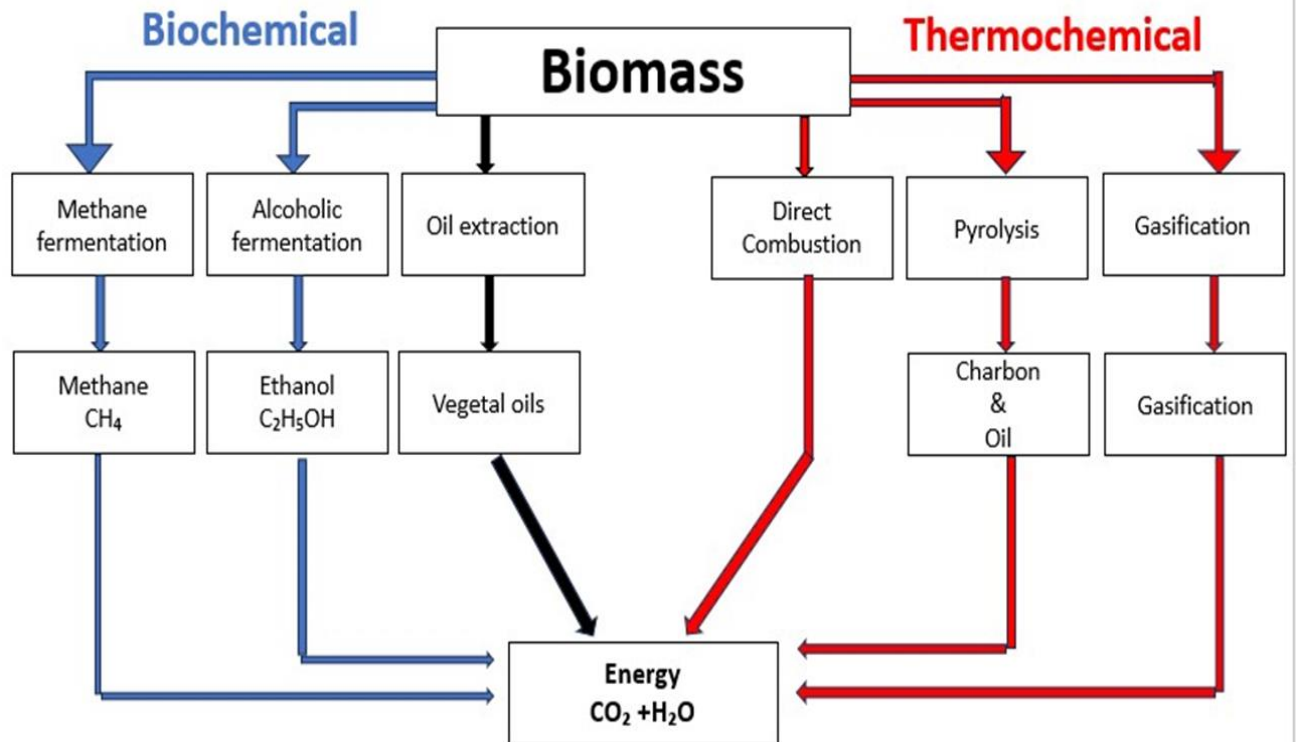


Figure I-6: Biomass conversion process. [14]

Biomass is defined as the “biodegradable fraction” of products, wastes and residues from agriculture, including plant and animal materials derived from the land and from seas, forests and related industries in addition to the biodegradable part industrial and domestic waste. All these organic materials can become a source of energy via combustion (such as wood energy), post-methanation, or biogas new chemical transformations. Biomass resources can be classified into several categories, according to which Origins: Wood in the form of logs, pellets and chips. Traditional agricultural products (cereals, etc.) and waste such as straw or biogasse (woody remains of sugarcane) and new plantations energy such as short-spinning branches (willow, miscanthus, etc.). Organic waste such as waste including sewage sludge, Domestic waste, and waste resulting from agriculture such as wastewater agricultural. [15]

I.4.4 Green Hydrogen

Hydrogen can be produced from various sources of raw materials including renewable and non-renewable sources which are around 87 million tons/year. Hydrogen is classified into different color shades i.e., blue, gray, brown, black, and green respectively based on their hydrogen production technology, energy source, and environmental impact as shown in (Table I-1) . [15]

Table I-1: Hydrogen color shades and their Technology, cost, and CO₂ emissions.[15]

Hydrogen Color	Technology	Source	Products	Cost (\$ kg/H ₂)	CO ₂ emissions
Brown Hydrogen	Gasification	Brown coal (Lignite)	H ₂ + CO ₂	1.2–2.1	High
Black Hydrogen	Gasification	Black coal (Bituminous)	H ₂ + CO ₂	1.2–2.1	High
Grey Hydrogen	Reforming	Natural gas	H ₂ + CO ₂ (Released)	1–2.1	Medium
Blue Hydrogen	Reforming + carbon capture	Natural gas	H ₂ + CO ₂ (Captured 85-95%)	1.5–2.9	Low
Green Hydrogen	Electrolysis	Water	H ₂ + O ₂	3.6–5.8	Minimal

I.5 A overview of some renewable heating projects

- Bahria et.al [16], the study compared solar heating and cooling systems in different regions of Algeria, using annual simulations to analyze the impact of high energy performance (HEP) buildings on heating and cooling loads (Figure I-7) compared to ordinary buildings. The results showed a reduction in total loads by 12%, 44%, and 22% in Algiers, Djelfa, and Tamanrasset, respectively. The solar fraction exceeded 45% in all cases with optimal parameters. Increasing insulation levels improved inside building temperatures by 4-5°C in winter. Heating loads decreased by approximately 58% in Algeria, 72% in Djelfa, and 12% in Tamanrasset for HEP buildings compared to ordinary buildings. Djelfa had the highest heating loads, while Tamanrasset had the highest cooling loads. Thermal inertia was crucial in winter but insufficient in summer where ventilation rate and sun protection played a role. The monthly solar fraction correlated with collector area, with optimal sizes identified for different regions. An optimal tilt angle of 35° for Djelfa and Algiers and 5° for Tamanrasset was recommended. The study concluded that applying solar heating and cooling systems in Algeria's regions is promising due to high solar potential, working year-round to reduce investment payback periods.

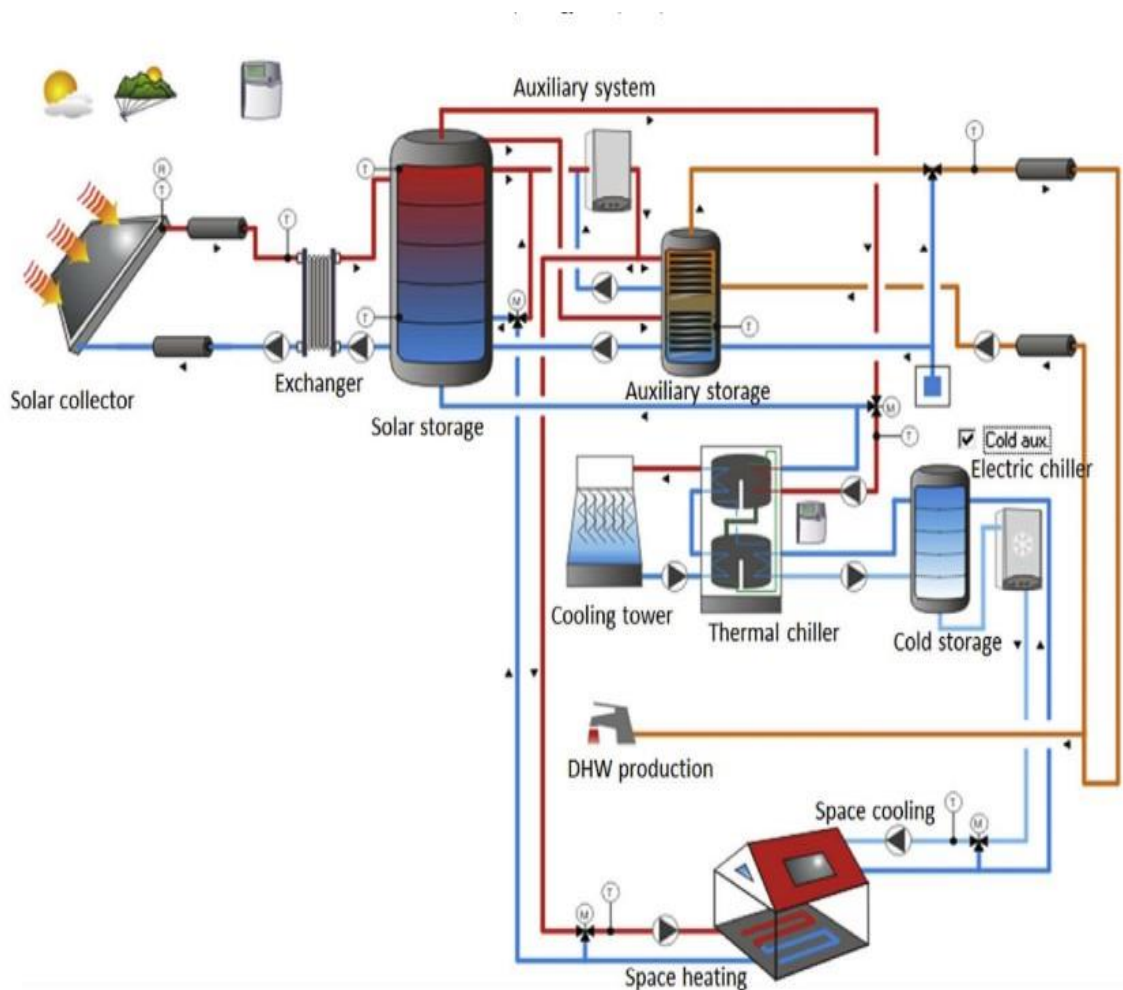


Figure I-7: A solar thermal system of DHW production, space heating and cooling. [16]

- Labeled et. al [17], applicability of solar desiccant cooling systems in Algerian Sahara, experimental investigation of flat plate collectors, studied the feasibility of a solar-powered solid desiccant system in Algerian Sahara, particularly in the region of Biskra, with low generation temperatures (50-80 °C). completed this study by an experimental performance evaluation of flat plate solar air heaters as an important component of the open-cycle dehumidification-humidification process. For the tested climatic conditions (T_{amb}=40 °C, RH=30 %), conclude that the air humidity in the building will be higher than the acceptable comfort conditions for the Pennington cycle. The solid desiccant cooling system can show a suitable blowing condition in the building when use the dynkel model, for the same climatic conditions. The major problem, which generally

can be an obstacle in the Sahara and particularly in the region of Biskra, is the applicability of the dynkel model in summer in very hot days ($T_{amb} \gg 40^{\circ}\text{C}$), which will be the subject of the future research. However, this study has also allowed to show that, the temperature achieved by the solar (FPCs) in a large band of air flow rate can satisfy the energy needs for the dehumidification of desiccant wheel. Thus, the produced and the stored hot water are in the operating temperature gap of these systems ($50\text{-}80^{\circ}\text{C}$).

- Abbas Ahmed in 2022 [18], a critical review on the use of shallow geothermal energy systems for heating and cooling discusses thermal energy storage, experimental investigation, specifically focusing on underground thermal energy storage systems (UTES) that use aquifers (ATES) or wells (BTES) to store thermal energy (Figure I-8). Underground thermal energy storage systems can store sensible heat by changing water temperature and some systems also incorporate latent heat storage. these systems are effective for heating and cooling buildings in Europe and north America, with (BTES) being particularly useful in areas with varying seasonal energy demands. (UTES) can store surplus solar and waste heat energy for later use, helping to balance energy supply and demand. And also mentions the first (BTES) system established in Sweden in 1983 and describes how (BTES) projects globally store solar energy in the summer for winter use. The process of charging and discharging a (BTES) involves circulating hot water through thermal zones in the well field.

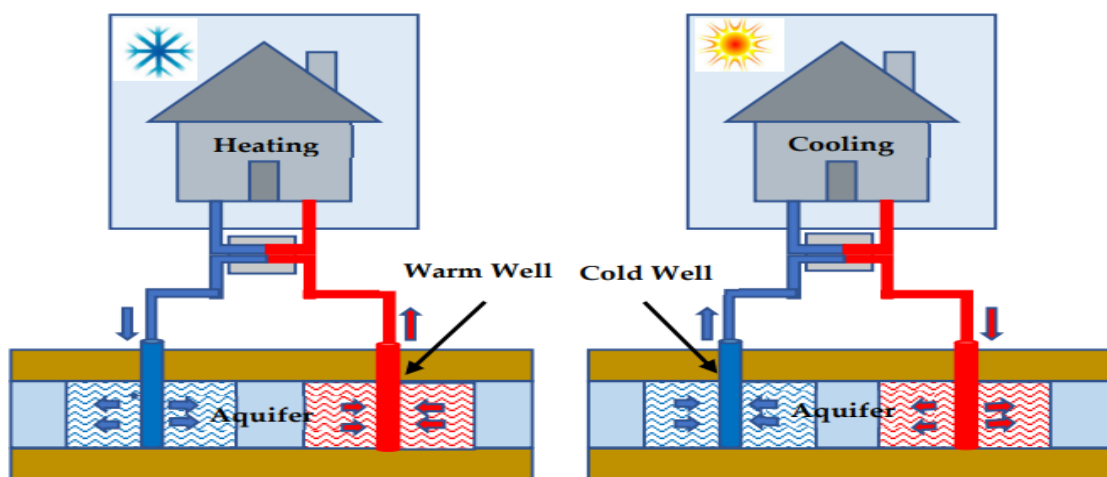


Figure I-8: Schematic of an Aquifer Thermal Energy Storage (ATES).[18]

- Romanov et. al in 2022 [19], represent the geothermal energy at different depths for district heating and cooling of existing and future building stock, numerical and experimental study, recent developments in the building sector, district heating and

cooling (DHC) field (Figure I-9 and Figure I-10), and geothermal technology are reported here, which indicate the trends and efforts to more sustainable and climate-friendly heating and cooling supply systems and may provide guidance for policymakers and decision-makers. The tendency towards lower temperatures in district heating networks and higher building envelope requirements are identified. meanwhile, technologies have been developed in the geothermal sector to reach deeper subsurface layers and to extract heat with higher temperature. to follow the progress in the building sector and (DHC), multi-faceted geothermal systems are considered here, which include components of deep, medium-deep and shallow geothermal resources. Because different temperatures occur at different depths, such a system can be used for different generations of (DHC) and buildings. This concept may be a part of an energy hub, and can help facilitate transformation from fossil fuel-based (DHC) to geothermal-based (DHC).

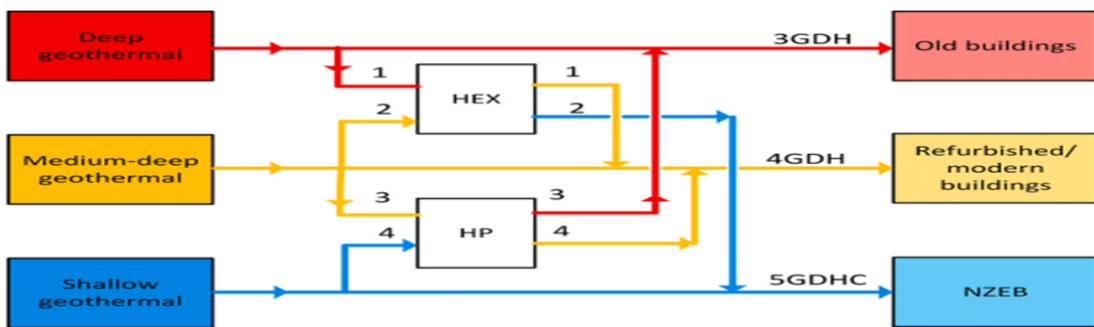


Figure I-9: Multi-faceted geothermal system.[19]

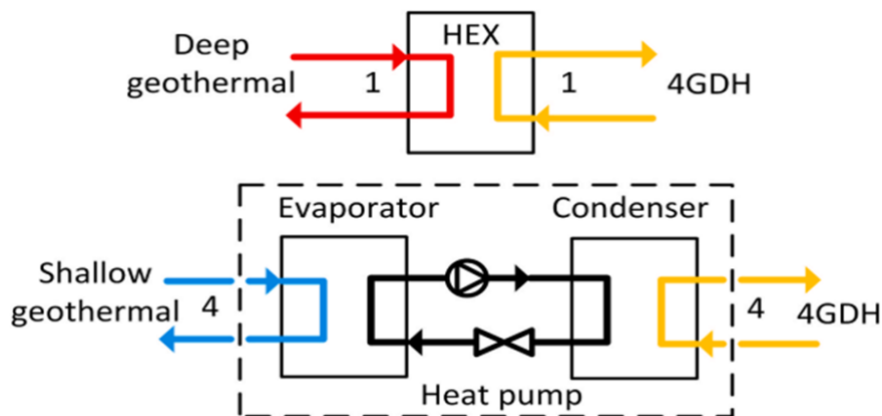


Figure I-10: Depicting heat transfer from deep geothermal system .[19]

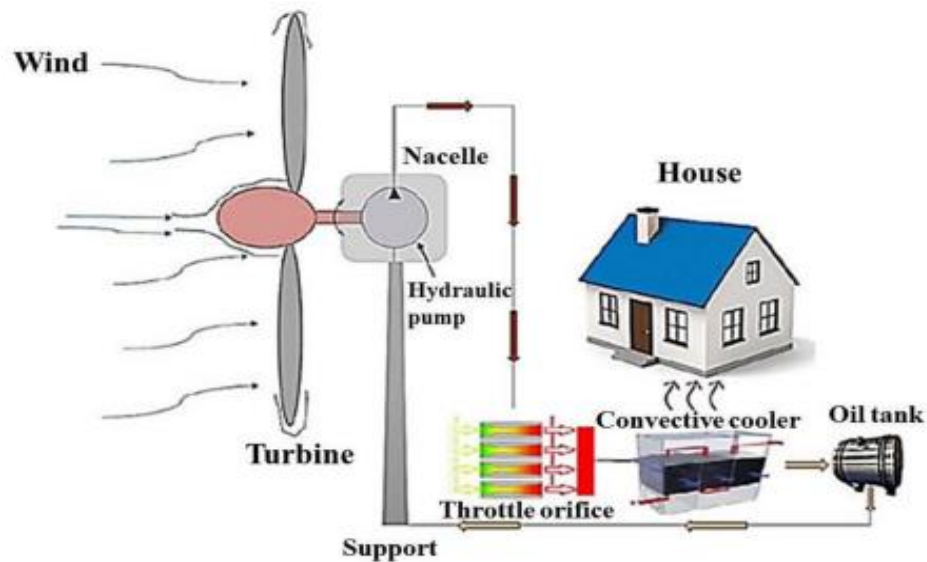


Figure I-11: Schematic of a novel domestic heating system. [20]

- Ravinder et. al in 2022 [20], a novel approach for direct conversion of wind energy to heat utilizing a hydraulic medium for domestic heating applications (Figure I-11). The objective of this scientific research was to investigate utilizing small to medium-scale wind energy in domestic heating without considerable losses by direct conversion of the wind energy to thermal energy through a hydraulic medium. For this purpose, the virtual wind turbine mathematical model was developed in Simulink. Using hardware-in-the-loop (HIL) simulation, the Simulink model was integrated with the (AC) motor connected to a variable displacement pump. the speed of the motor was controlled using a frequency converter, to which the torque of the virtual turbine model was supplied in real-time, and the angular velocity of the motor was fed back to the system ,by regulating the valve orifice, a pressure drop was created across the orifice area, which led to the generation of thermal power. In order to validate the real-time simulated turbine, the output power and the characteristic curve of the tip speed ratio (λ) based on the power coefficient (CP) resulted from the real-time simulation were reconciled with the corresponding curves of the real turbine. The results demonstrated the conformity of the real-time simulation with the real turbine. The thermal power produced was measured by measuring the temperature of the hydraulic oil.

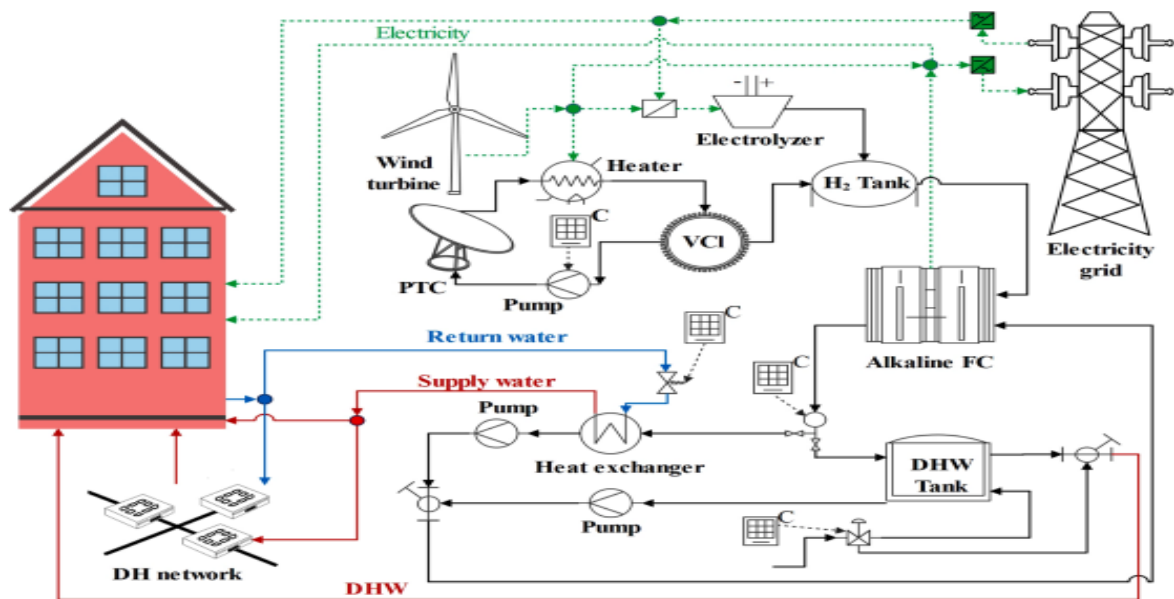


Figure I- 12: A graphical illustration of the proposed smart building energy system driven by renewable sources.[21]

- Behzadi et.al in 2023[21], they conducted scientific research on a rule-based energy management strategy for a low-temperature solar/ wind-driven heating system optimized by the machine learning-assisted (FigureI-12). this research discussing the smart building energy system innovative, practical, and cost-effective solution for developing intelligent building energy systems and supporting the intended global green transition with maximum renewable integration. The vanadium chloride cycle, electrolyzer unit, and alkaline fuel cell are powered by solar and wind energy to produce/store/use hydrogen. A rule-based control scheme is designed to provide a sophisticated interplay between the demand/supply sides, components, and local energy networks to reduce peak capacity, lower emissions, and save energy costs.
- Dridi et.al in 2015 [13], experimental study about estimation of potential biomass in Algeria. The biomass potential in Algeria is about 3.7 million (TEP) which comes from forests and 1.33 million (TEP) per year, from agriculture and urban waste, this potential unusable until today. Biomass conversion technology at the national institute of agriculture (INA) in harrach (Alegria) established a facility to produce combustible gas (biogas) in from agricultural waste. evaluated the potential of vegetable residues (Olive waste) in northern Algeria: it was proposed to install a unit with a capacity of 6 megawatts Béjaïa. 70,000 tons of olive waste annually to produce Nearly 45 GWh/year.

- Guerrout et.al in 2022[22], experimental study and numerical simulation of naturel ventilation in building partner with solar chimney and solar tower study (Figure I-13) energy sectors are responsible for most of the greenhouse gas emissions in the world. A significant amount of energy is consumed by the residential sector in hot and semi-arid regions, which clearly shows the importance of developing sustainable energy technologies for this sector. the objective of this work is to study the behavior and dynamic performance of a solar chimney coupled with a wind tower, an experimental study was carried out, based on the measurement of physical parameters at the input and output of both systems. as well as a numerical study that was conducted after obtaining the experimental results. the numerical calculation is carried out using the simulation software Ansys 2021 version R1. the correct choice of the installation position of both systems is able to improve the distribution of the air flow inside the cell, in addition to the fact that the increase in the speed at the entrance of the wind tower allows to generate the air renewal rate (ACH) approximately 25.6 1/h at an average speed of 2.5 m/s. the results show that both systems are effective in creating natural ventilation. Selection of the position of the solar chimney and wind tower plays an important role in obtaining the best air velocity distribution in the room. Five different configurations were proposed for the studied model. the air speed at the entrance to the wind tower was 0.2 m/s. the results showed that the best airflow distribution was in the fourth configuration, where the mass flow value was 0.0348 kg/s and the ACH value was equal to 4.26 1/h.

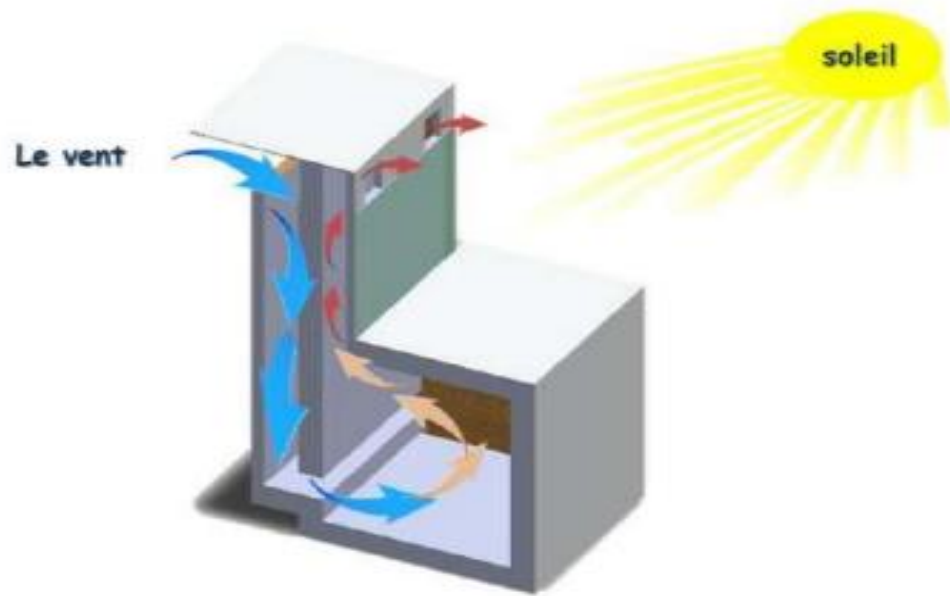


Figure I-13: Physical model of solar chimney [22]

- Zelaci et. al in 2022 [23], optimization and numerical simulation of a new cooling by an air-to-ground heat exchanger coupled with a wind tower in an arid climate (Figure I-14). The aim of the study is to achieve passive cooling using an air-to-ground heat exchanger linked to the wind tower system . First, a simulation-based optimization approach and the Taguchi method are applied to obtain the optimal dimensions of the wind tower under the borgla sieves. A three-dimensional digital simulation of the heat exchanger and the ground coupled to the wind tower was performed using the fluent program for a year. The results obtained showed a good temperature contrast between the inlet and outlet of the system, as it was estimated in the summer to be 9.4°C. in the winter, it was 84.15. After determining the system, became clear that it reached 68% in the summer period in the winter period 80%.

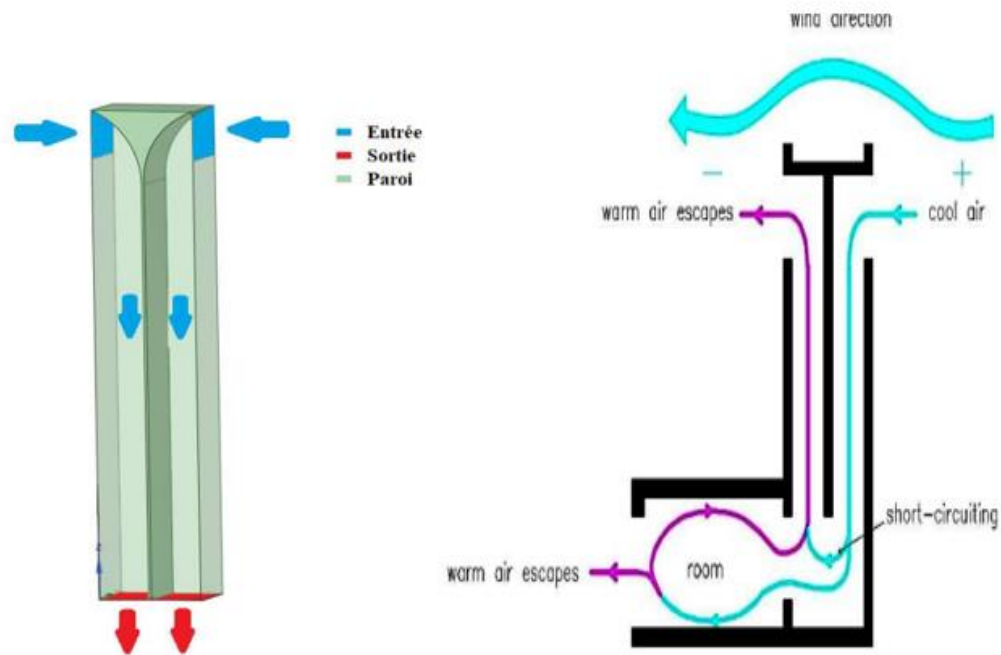


Figure I -14: Wind Towers. [23]

- Wang et al. in 2015[24], a CFD simulation of 3D Air flow and temperature variation in refrigeration cabinet (Figure I-15). Summarize simulation of airflow and temperature fluctuations during operation of an ice beverage refrigerator automatic dynamic opening and closing cycles. In order to correctly simulate the effect of a porous plate separating the evaporator and the storage chamber, a benchmark problem was designed and used as a reference to determine the parameters in the porous jump model through parameter optimization. subsequently, the dynamic cycle of the first power-on, automatic shutdown and automatic power-on were simulated. The flow field distribution and temperature distribution were analyzed and the time required for these three stages was determined. the complete 3D CFD simulation of the cooling system not only provides a detailed temperature distribution inside the cabinet, but also provides the operating parameters of the system, such as B. for opening and closing cycles. These results simulation is very important for cabinet design to improve the storage quality of products while reducing energy consumption.

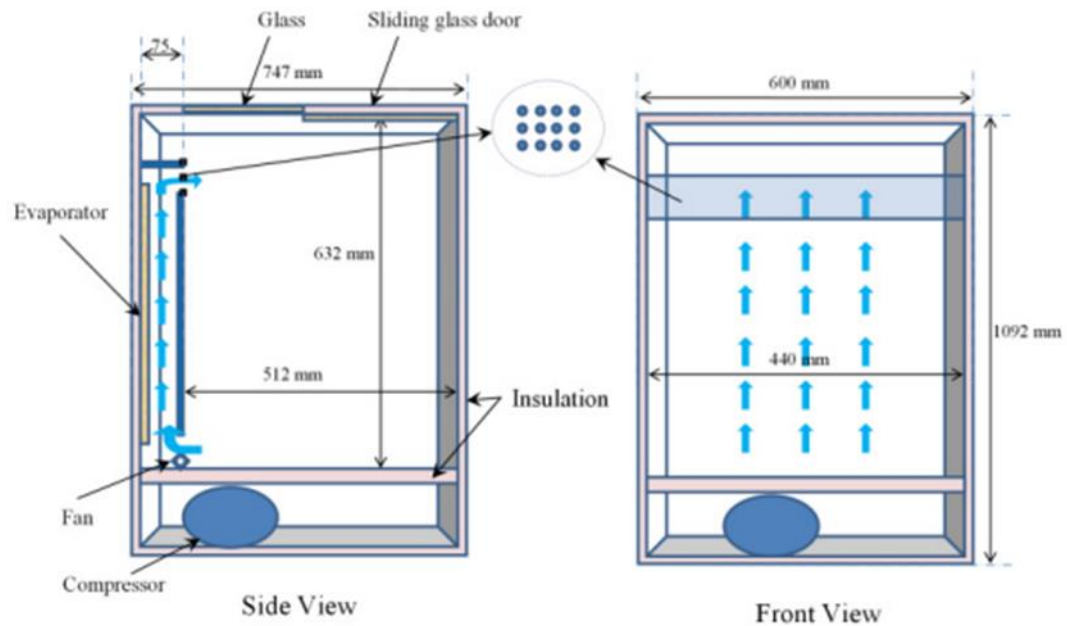


Figure I -15: The sketch of the simulated refrigeration cabinet. [24]

- Study of a passive solar winter heating system based on trombe wall by Narasimham et al. in 2016[25], taken in this analysis numerical study on the passive solar winter heating system. study the distribution of temperature in wall, living space of room and the effect of outlet position, propose three levels (Outlet vents at the top position, middle and at bottom), two software packages (GAMBIT) and (ANSYS FLUENT) version.6.3.26 is used for create 2-D models. (Figure I-16). The results are obtained by varying the quantity of heat flow and temperature showed that the efficiency of the winter heating system can vary with the position of the outlet vent. in winter heating system the outlet position at bottom is better compared top and center.

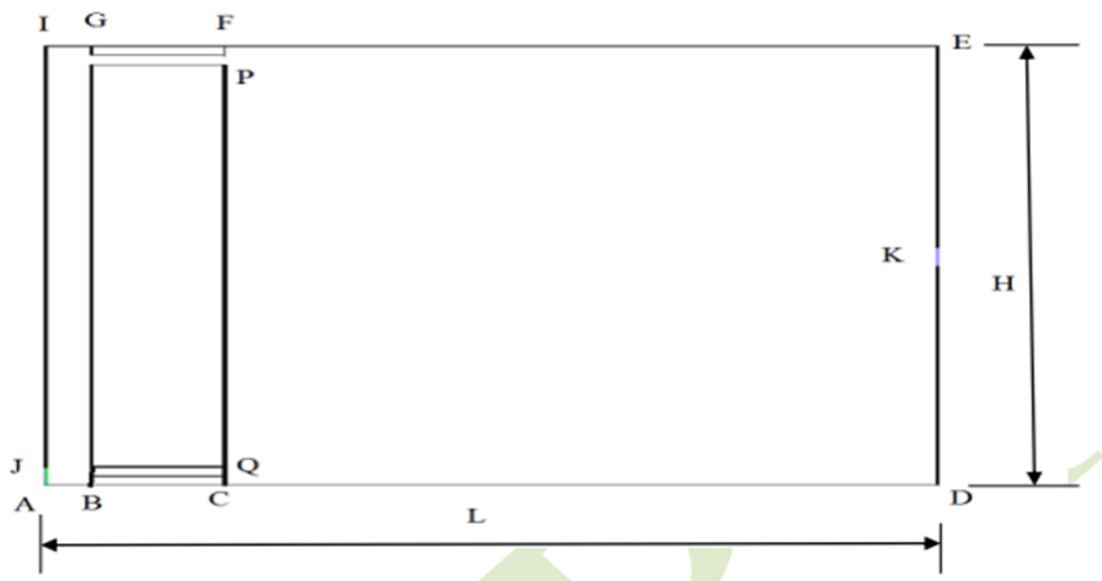


Figure I-16: physical model for winter heating system in 2D. [25]

I.6 Conclusion

Renewable energy-based heating systems are witnessing significant developments, with technologies like solar heating and geothermal heating becoming more prevalent and efficient. Advancements in energy storage and smart control systems are also progressing, enhancing usage efficiency and reducing energy consumption. Continued innovation and investment are expected to bring further progress and improvement in this field.

Chapter II

Mathematical modeling of a heating system for a living room

II.1 Introduction

This chapter highlights the importance of understanding thermal behavior in buildings and provides an overview of the expected range of content. It also analyzes thermal fundamentals such as heat transfer and material properties, and reviews mathematical modeling techniques to analyze these behaviors. It also discusses the importance of boundary conditions and correct interventions, and sheds light on methods for verifying and validating models. In addition, researching how to incorporate ambient atmospheric data into the modeling process to achieve better accuracy. In conclusion, we discuss practical applications and typical cases to illustrate the uses of modeling in this field.

II.2 Presentation of the study region

Ouargla region is located in southeastern Algeria (Figure II-1), about 800 kilometers from the capital, Algiers. Ouargla, the capital of state Province, is 157 meters above sea level, with geographical coordinates of $31^{\circ}58'$ north latitude and $5^{\circ}20'$ east longitude. The province of Ouargla covers an area of 163,263 km². [26]



Figure II-1: Wilaya of Ouargla, Algeria. [27]

II.3 Climate data

II.3.1 Solar radiation (W/m^2) for the Ouargla region 2023-2019. [28]

The corresponding curve (Figure II-2) represents the average solar radiation for 5 years (2019-2023) in the city of Ouargla, where notice that in January lowest value (151.7 W/m^2), then it gradually increases at February and March from (188.9 W/m^2) to (233.3 W/m^2), close value about ($299\text{-}300 \text{ W/m}^2$) in May and June, then the radiation reaches the highest value in July (322.7 W/m^2) then decreases in the next months from (246 W/m^2) to (136.5 W/m^2).

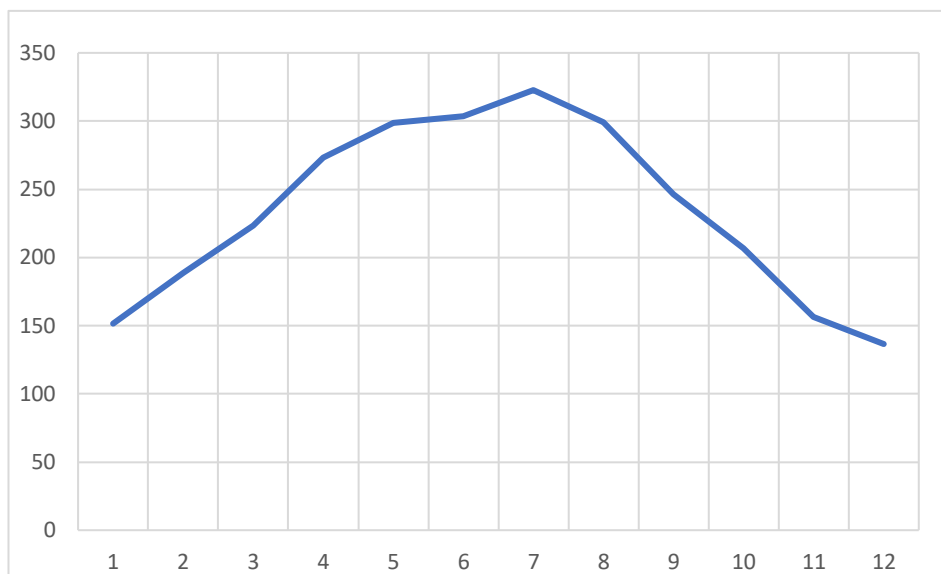


Figure II- 2: Solar radiation data

II.3.2 Temperature (C°) Data for the Ouargla region 2023-2019. [28]

Curve of average temperature changes (Figure II-3) for 5 years (2019-2023) in Ouargla region, in the winter months (December, January, February) the temperature was low (13.43 C° to 14.28 C°) and in spring (March, April, May) gradually between (18.62 C° - 28.89 C°) then reaches its highest value at summer (June, July, August) to (37 C° - 36 C°) and start decreases during the fall months (September, October, November) between (24.93 C° - 13.43 C°).

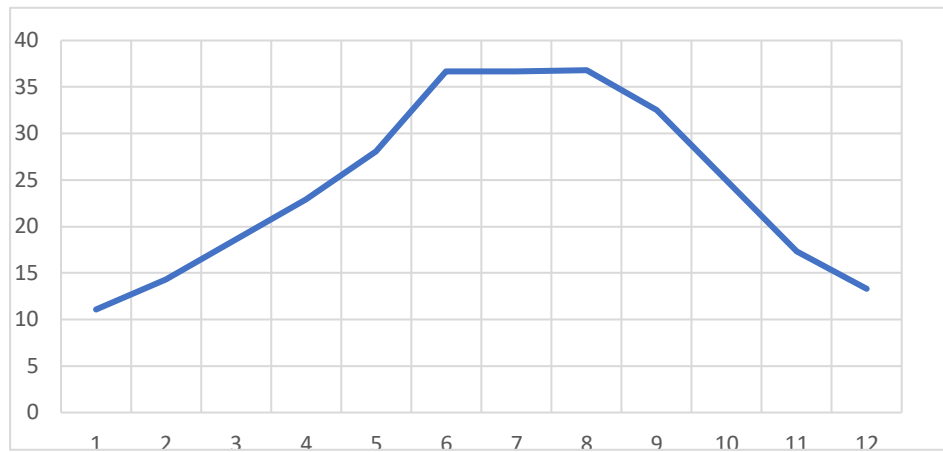


Figure II-3: Temperature (C°) Data

II.3.3 Wind Speed data (km/h) for Ouargla region 2019-2023.[28]

The (Figure II-4) represents months and wind speed (Km/h) in the terms of months of the year for 5 years (2019-2023) in Ouargla region , notice in the winter (December ,January, February) close value about(3 Km/h to 3.9 Km/h) and in spring (March, April, May) the wind speed almost constant (4.46 Km/h) then gradually increases from (4.56 Km/h) to (3.62Km/h) at summer (June, July, August), and rises during the fall months (September, October, November) to (3.88Km/h -3.18Km/h).

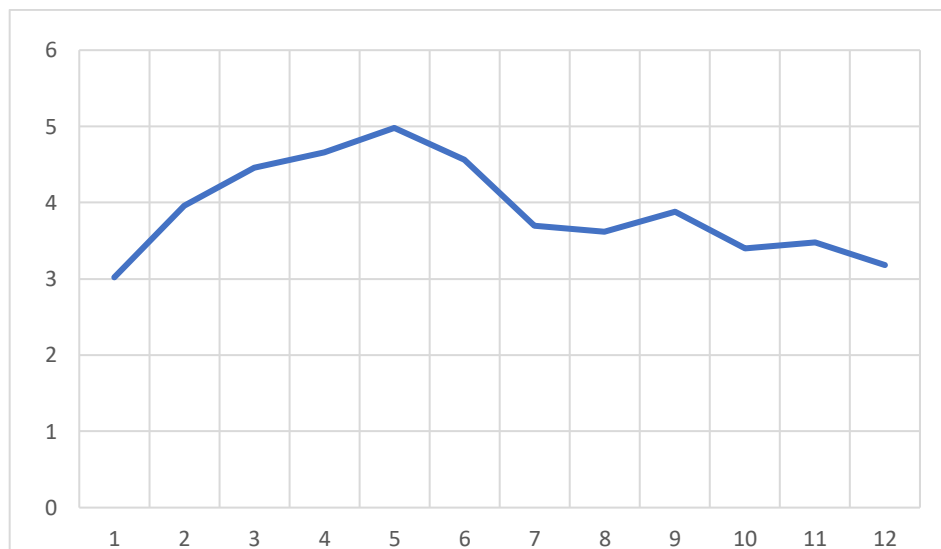


Figure II- 4: Wind speed data

II.3.4 Humidity (%) data for Ouargla region 2019-2023. [28]

Humidity (%) changes during 5 years (2019-2023) for Ouargla region (figure II-5) where notice that in the winter (December, January, February) the humidity relatively high about (43.14%), and in spring (March, April, May) is constant (25%) increases at summer

(June, July, August) from (15.98%) to (25.42%) and rises during the fall months (September, October, November) between(32 % -49.3%).

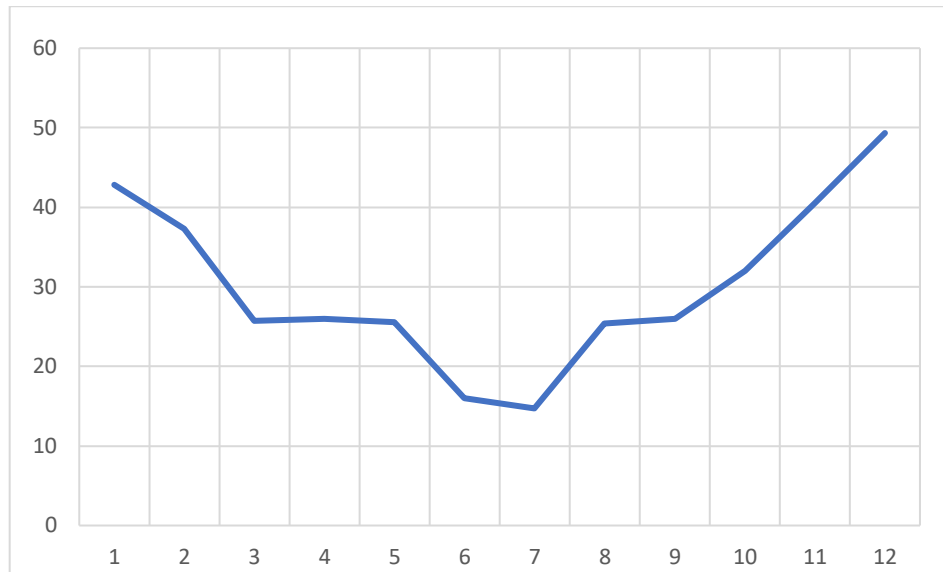


Figure II-5: Humidity data.

II.4 Modeling the thermal behavior of building component

In the corresponding table (Table II-1) characteristics of the building components and type of material used in each of them, where we compare material, thickness, thermal conductivity and density for each of the wall, roof, ground floor, window and door.

Table II-1: Characteristics of building elements

Envelope Element	Material	Thickness (m)	Thermal conductivity(w/m*k)	Density (kg/m ³)
Wall	Cement plaster	0.20	1.413	849
	Brick	0.150	0.690	1920
	Plaster	0.020	0.700	849
	Cement plaster	0.20	1.413	849
Roof	Rib and Brick slab	0.200	0.690	1580
	Plaster	0.020	0.700	2778
	Granite tile	0.025	2.99	0.00275
Ground floor	Cement plaster	0.020	1.413	849
	Backfill	0.200	0.8	0.00192
	Frame		0.13	25000
Window	Single glass	0.02	0.65	2500

Door	Wood	0.04	0.13	352
------	------	------	------	-----

II.5 Modeling the thermal behavior of a building

Heat is considered one of the most important types of energy for humans. In buildings for example, the transfer of thermal energy is one of the problems we face when constructing buildings. This chapter deals with the study of thermal performance and energy consumption in 2D of turbulent flow in real time of compressible fluid and stationary dynamics, that is modelling and understanding the thermal behavior of buildings. [29]

II.5.1 Model of a wall without insulation

A wall can be modeled by the ordinary differential equation

$$\frac{dT_w}{dt} = \frac{A_w}{C_w} [U_{wi}(T_{ai} - T_w) + U_{wo}(T_{ao} - T_w)] \quad \text{II 1}$$

II.5.2 Model of a window without insulation

The window is modeled by the ordinary differential equation

$$Q_g - air = A_g U_g (T_{ao} - win - T_{ai}) \quad \text{II 2}$$

II.5.3 Model of a door without insulation

The model of a door takes into account the heat exchange between the temperature of the door and of the parts that it separates it is modeled by the equation

$$C_{sd} \frac{dT_d}{dt} = U_d [(1 + \alpha_d)(T_{aiA} - T_d) + (1 - \alpha_d)(T_{aiB} - T_d)] \quad \text{II 3}$$

II.5.4 Model of a ceiling without insulation

The ceiling is one of the components of the building; its temperature is assumed uniform. The model of the ceiling of a room is given by equation

$$\frac{dT_c}{dt} = \frac{A_c}{C_c} [U_{ci}(T_{ai} - T_c) + U_{co}(T_{ao} - T_c)] \quad \text{II 4}$$

II.5.5 Model of a heated floor

The floor is a heating element of the building, it is modeled by the equation

$$\frac{dT_f}{dt} = \frac{A_f}{C_f} \left[P \frac{Q_s}{A_f} + U_f (T_{ai} - T_f) + \frac{Q_{water}}{A_f} \right] \quad \text{II 5}$$

II.6 Room ambient temperature model

The evolution of the air temperature in a room is given by the ordinary differential equation

$$\frac{dT_{ai}}{dt} = \frac{1}{C_a} [Q_e + A_g U_g (T_{ao} - T_{ai}) + A_{ws} U_{ws} (T_{ws} - T_{ai}) + A_{wn} U_{wn} (T_{wn} - T_{ai}) + A_{we} U_{we} (T_{we} - T_{ai}) + A_{woe} U_{woe} (T_{woe} - T_{ai}) + A_f U_f (T_f - T_{ai}) + A_c U_c (T_c - T_{ai})] \quad \text{II 6}$$

II.7 GOVERNING EQUATIONS IN 2D

- Continuity equation [30]

$$\frac{\partial u}{\partial x} + \frac{\partial v}{\partial y} = 0 \quad \text{II 7}$$

- X-direction momentum equation [30]

$$u \frac{\partial u}{\partial x} + v \frac{\partial u}{\partial y} = -\frac{1}{\rho} \frac{\partial p}{\partial x} \quad \text{II 8}$$

- Y-direction momentum equation [30]

$$u \frac{\partial v}{\partial x} + v \frac{\partial v}{\partial y} = -\frac{1}{\rho} \frac{\partial p}{\partial y} + \nu \nabla^2 v - [1 - \beta (-T_1)] \quad \text{II 9}$$

- Fluid energy equation [30]

$$u \frac{\partial T}{\partial x} + v \frac{\partial T}{\partial y} = \alpha \nabla^2 T \quad \text{II 10}$$

- Heat conduction equation in the thermal storage wall [30]

$$\nabla^2 T_w = 0 \quad \text{II 11}$$

II.8 BOUNDARY CONDITIONS

The hydrodynamic boundary conditions are no-slip conditions on all the rigid wall surfaces and atmospheric pressure at the openings on the external walls. The thermal boundary conditions are as follows:

Air entering the enclosure through an opening on the external wall is assumed to be at T_1 .

Air leaving any opening on an external wall is assumed to obey the zero gradient condition,

$\frac{\partial T}{\partial x} = 0$ On the vertical side of the thermal storage wall exposed to solar radiation, the interface condition is. [30]

$$q_s = -k \frac{dT(O,t)}{dx} = 0 \quad \text{II 12}$$

The above interface condition states that the solar radiation flux q_s is partly conducted into the air in the chimney (first term on the right-hand side) and partly into the thermal storage wall (second term on the right-hand side). Here it should be noted q_s is the net (or effective) solar radiation flux that remains after passing through the glazing. This flux falls on the side of the thermal storage wall exposed to the sunlight side. The other vertical surface of the thermal storage wall is in communication with the room air and does not receive any flux from external side. Hence, the interface condition for this surface becomes:

$$kw \frac{\partial T_w}{\partial x} = k \frac{\partial T}{\partial x} \quad \text{II 13}$$

All other surfaces of part surfaces, horizontal or vertical are assumed adiabatic, on these walls:

$$\partial T \frac{\partial T}{\partial n} = 0 \quad \text{II 14}$$

Where n represents either x -coordinate or y -coordinate, as the case may be. The thermal boundary conditions give rise to another dimensionless parameter, namely, kw/k . This is the thermal conductivity ratio of the wall to that of air. After non-dimensionalization. The interface conditions become:

$$1 = \frac{\partial \theta}{\partial x} - \frac{Kw}{K} \frac{\partial \theta_w}{\partial x} \quad \text{II 15}$$

On the radiation side of the thermal storage wall

$$\frac{\partial \theta}{\partial x} = - \frac{Kw}{K} \frac{\partial \theta_w}{\partial x} \quad \text{II 16}$$

and on the wall-room-air interface. The adiabatic conditions become:

$$\frac{\partial \theta}{\partial N} = 0 \quad \text{II 17}$$

Where N is either X or Y . Apart from the above, we have number dimensionless geometrical parameters such as H/L .

II.9 Conclusion:

At the end of this chapter, we extract the heat transfer equations in the building elements and mention the heat transfer equations in living room 2D with the boundary conditions of the Trombe wall.

Chapter III

Simulation Results.

III.1 Introduction

This chapter presents a simulation of the trombe wall in fluent and gambit program where it performs the analysis of a two-dimensional (2D) model (Figure III-1) with dimensions in (table III-1). The work includes the thermal mode of heat transfer in the presence of three different outlet position in the system and track changes of velocity and temperature in the room

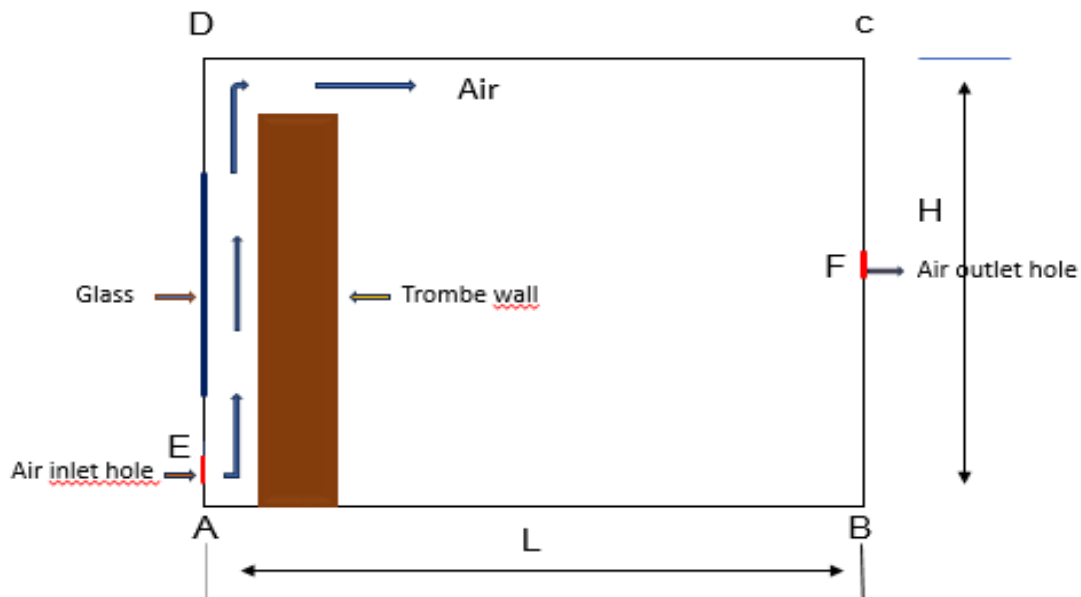


Figure III -1: Physical model for heating system in 2D.

Table III-1: Trombe Wall model dimensions.

Parameters	Dimensions(m)
Concrete wall width	0.3
Concrete wall height	2.4
Room length	3
Room height (H)	4
Glass thickness	0.06
Air space	0.1
width of opening	0.1

In fluent program, we have entered settings and their model (Table III -2), the first setting (density) to consider buoyancy effect and the second (energy) to consider heat transfer

Table III -2: Settings and model in fluent program.

Setting	Model	Reason
Density	Boussinesq approximation	To consider buoyancy effect
Energy	Activated	To consider heat transfer

The table shows (Table III-3) three zone type and their continuum Condition in fluent program.

Table III-3: Zones type and continuum Condition in fluent program.

zone type	continuum condition
Brick wall	solid
Room interior	fluid
Air space	fluid

The table shows (Table III-4) zones type(glass , brick wall (hs) ,inlet , outlet , roof, ground floor, wall openings) and their boundary condition in fluent program.

Table III-4: Zones type and boundary condition.

zone type	boundary condition
glass	Wall
Brick wall (hs)	Wall
inlet	pressure inlet
outlet	Pressure outlet
Roof	Wall
Ground floor	wall
Wall openings	interior

We entered transaction of factors (pressure, body force, density, momentum and energy) shown in the following table (Table III-5)

Table III-5: Factors in fluent program

PRESSURE	0.3
BODY FORCE	1
DENSITY	1
MOMENTUM	0.7
ENERGY	1

III.2 Grid size test

We used four different mesh sizes in our work (0.1 ,0.05 ,0.01 ,0.005) and we compare her cells, faces and nodes (Table III-6) , to choose the best mesh size to work with .

Table III-6: Mesh size used in our work.

Mech	0.1	0.05	0.01	0.005
Cells	720	2880	72000	288000
Faces	1542	5964	145020	578040
nodes	821	3083	73019	290039

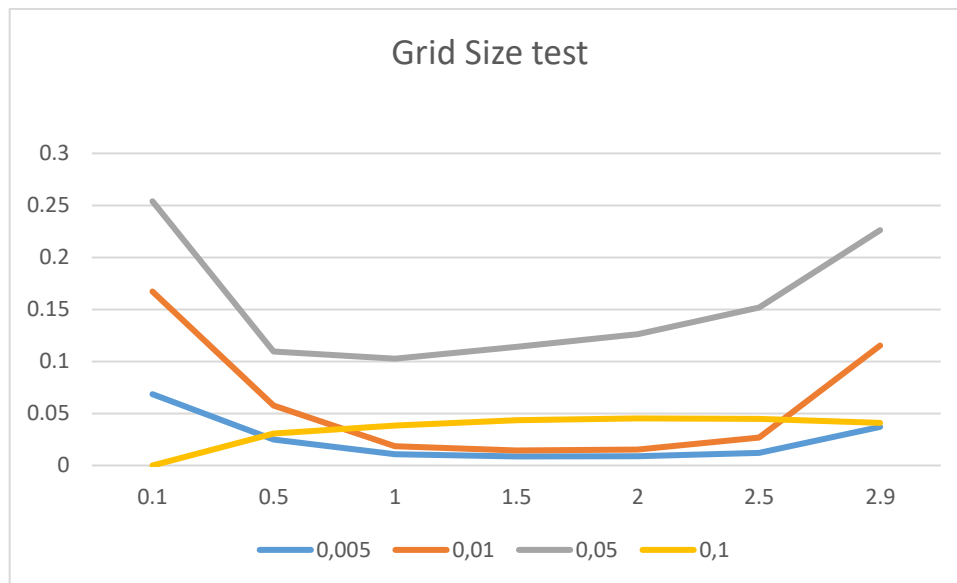


Figure III-2: Grid size test.

This curve in (Figure III-2) represents changes in airspeed as a function of distance in several cases, we are about to model a room with a trombe wall in the program GAMBIT, FLUENT. with changing the position of the outlet (top, middle, bottom) every time we change size match it to four points (0.1/0.05/0.01/0.005) (Table III-6), then we run the simulation in a program FLUENT and then the results show us that point (0.01) is the best point, so we can do the rest of the study on it in the rest of the output locations.

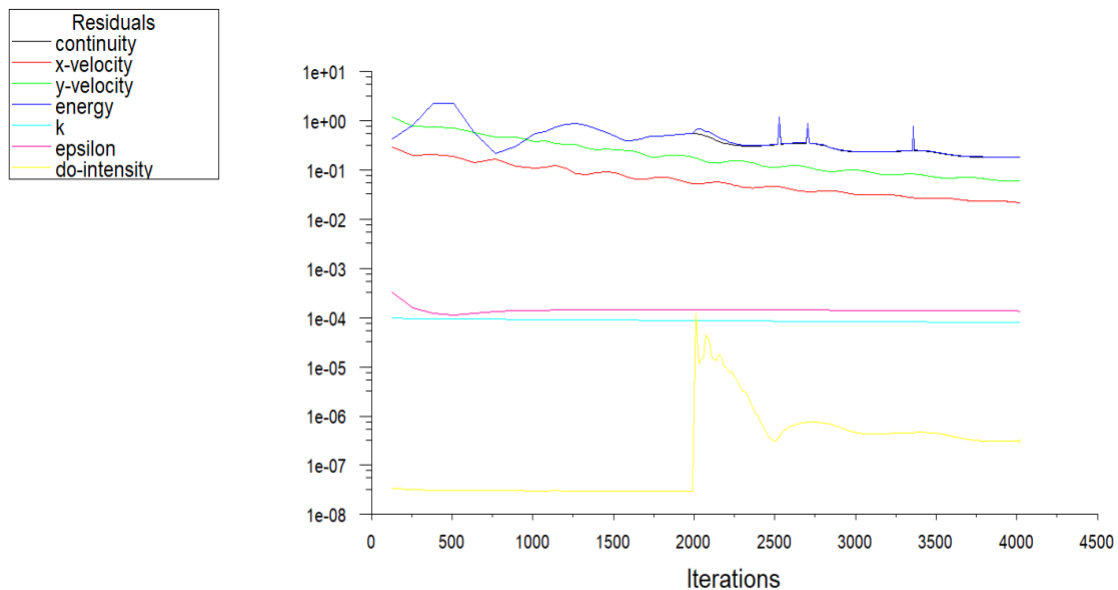
III.3 Solution control (convergence)

Fluent program reports a residual for each governing equation being solved (Table III-7), the residual is a measure of how well the current solution satisfies the discrete form of each governing equation. we'll iterate the solution (1000 iteration) until the residual for each equation (continuity, velocity to-x, velocity to-y, K-e) falls below 10^{-4} and energy equation to 10^{-6} , after finish iteration we find the solution control (convergence curve) (Figure III-3).

Table III-7: The residuals for the governing equations.

Equation	Velocity according to X	Velocity according to Y	Equation of continuity	Equation of energy	K	epsilon

Residue	10^{-4}	10^{-4}	10^{-4}	10^{-6}	10^{-4}	10^{-4}
---------	-----------	-----------	-----------	-----------	-----------	-----------



Scaled Residuals

May 29, 2024
FLUENT 6.3 (2d, dp, dbns imp, rke)

Figure III-3: Convergence Curve.

III.4 VALIDATION OF RESULTS

The numerical model has been validated by previous research conducted by Narasimham et al. in 2016[25], we compared and analyzed the numerical results presented by Narasimham et al. in 2016[25] with the results obtained from our numerical model under the same condition with changing the wall material (they used a concrete wall and we replaced it with a brick wall) and the residuals for the governing equations (they used residual for all variables is 10^{-6} and we used residual for each equation (continuity, velocity to-x, velocity to-y, K-e) falls below 10^{-4} and energy equation to 10^{-6}).

The current results show that our numerical results are in broad agreement with the numerical results of Narasimham et al. in 2016[25].

III.5 RESULTS AND DISCUSSIONS

(Figure III-4) represents the temperature ($^{\circ}\text{C}$) changes in a room equipped with a trombe wall with dimensions (4m x 3m) in the case of the outlet at the top, where we notice that the

temperature enters the room from the lower entrance in the trombe wall with the value ($4.86 \times 10^{+1}$) where we notice the temperature is hottest at the tromps wall between (5.33×10^1) to ($4.7 \times 10^{+1}$) and as we move away from the wall we notice a decrease in the temperature in the interior space between ($3.15 \times 10^{+1}$ C°) to (2.68×10^{-1} C°).

III.5.1 Top outlet

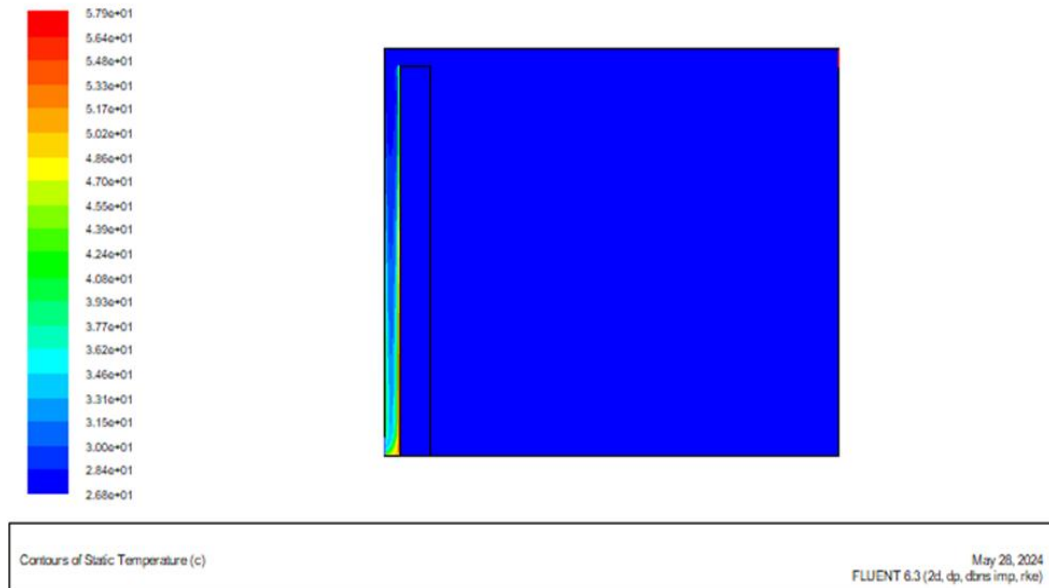


Figure III-4: Contours of static temperature (C°) [TOP Outlet 0.01].

(Figure III-5) represents the changes in air speed (m/s) in a room equipped with a trombe wall with dimensions (4mx3m) in the case of an outlet at the top, where we notice that at the air entry point the speed is average between (9.50×10^{-2} m/s) to (1.90×10^{-1} m/s) then it begins to accelerate at the upper opening of the trombe wall until it reaches the maximum speed (2.71×10^{-1} m/s) then it begins to decrease again until it reaches the upper vent opening on the right wall. We also notice that the air does not move in the inner space of the room.

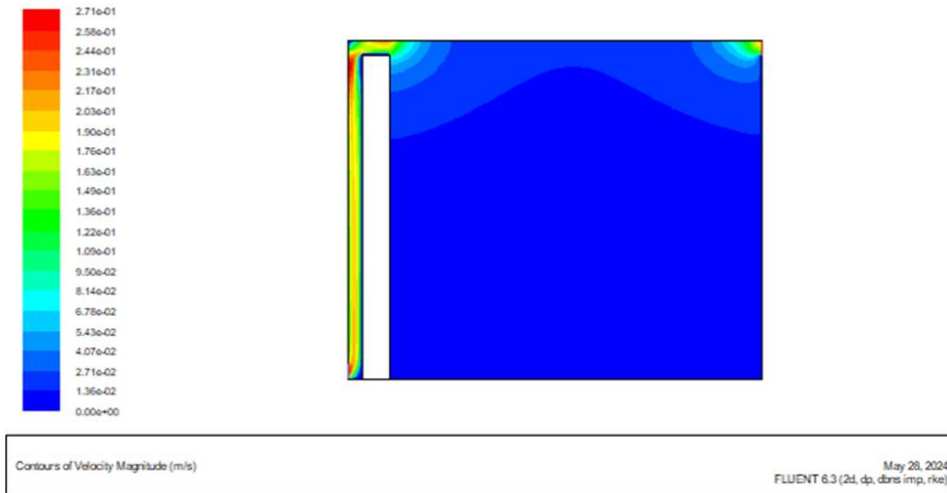


Figure III-5: Contours of static Velocity (m/s) [TOP Outlet0.01].

The curve in (Figure III-6) represents the changes in airspeed as a function of the location close to the upper air-breathing point. We notice that the air speed starts from a very small speed (6×10^{-2} m/s) and then increases gradually until it reaches at the value (2×10^{-1} m/s) and then returns to decreasing suddenly until the point (5.5×10^{-2} m/s)

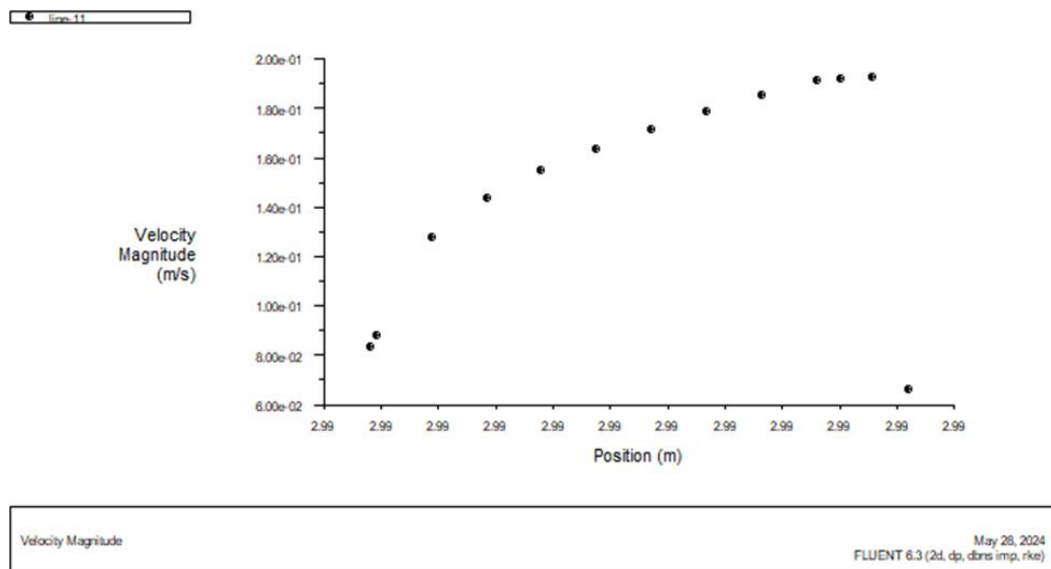


Figure III-6: Velocity change curve as a function of distance.

The (Figure III-7) represents contours of static temperature in a living room equipped with a trombe wall case of vent outlet in middle of the wall. we notice that the temperature starts from a high value between two degrees ($4.73 \times 10^{+1} \text{ C}^\circ$)/($3.86 \times 10^{+1} \text{ C}^\circ$) and it gradually decreases when go upper the trombe wall about ($3.86 \times 10^{+1} \text{ C}^\circ$) and lowest temperature inside the space room has a value ($2.69 \times 10^{+1} \text{ C}^\circ$).

III.5.2 Middle outlet

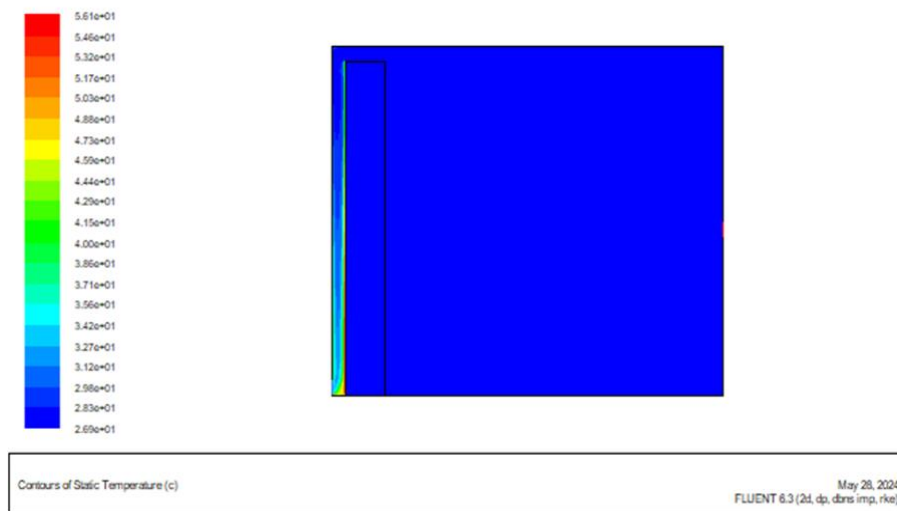


Figure III-7: Contours of static temperature (C°) [middle Outlet0.01].

(Figure III-8) represents the changes in air velocity in a room equipped with a trombe wall with dimensions (4mx3m) in the case of the air outlet in the middle of the wall, where we notice that the air speed is average at the entry point at the bottom of the trombe wall between ($2.50 \times 10^{-1} \text{ m/s}$) to ($1.56 \times 10^{-1} \text{ m/s}$) then it begins to accelerate uniformly at the speed ($2.18 \times 10^{-1} \text{ m/s}$) until it reaches the highest speed at the upper opening after the trombe wall at the speed ($3.12 \times 10^{-1} \text{ m/s}$) and then it gradually decreases until the air reaches the vent in the middle of the opposite wall at the speed between ($1.87 \times 10^{-1} \text{ m/s}$) to ($1.25 \times 10^{-1} \text{ m/s}$).

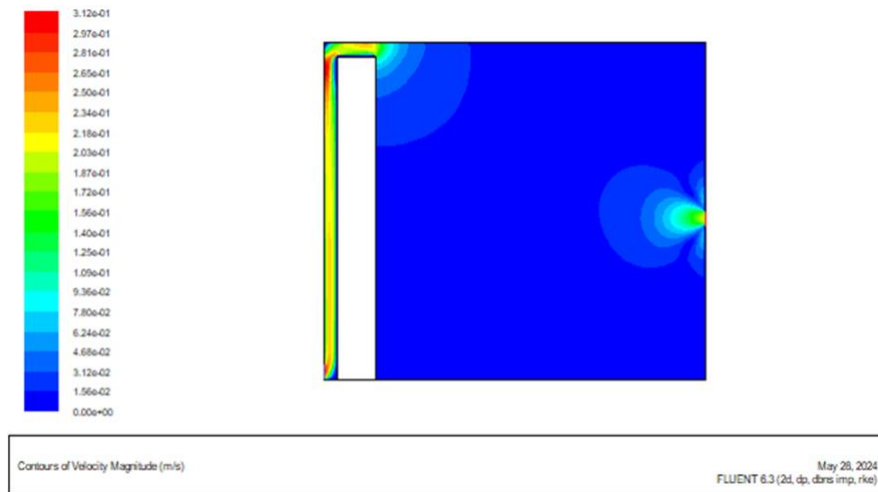


Figure III-8: Contours of static velocity (m/s) [middle Outlet0.01]

The curve in (Figure III-9) represents the changes in air speed as a function of location in the living room equipped with a trombe wall. We notice that the air speed starts at a low value at (0.170m/s) and then begins to increase regularly until it reaches the highest value at (1.97m/s) then it decreases gradually until it stabilizes at the value (0.150m/s).

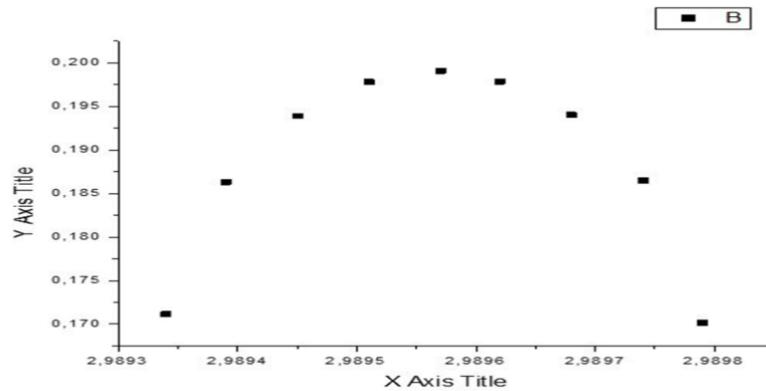


Figure III-9: Velocity change curve as a function of distance

The Contours in (Figure III-10) represents of temperature changes in a living room equipped with a trombe wall with a vent outlet at the bottom. We notice that the temperature starts from a very low point at the entry point at the bottom of the trombe wall, between $(4.77 \times 10^1 \text{m/s})$ and $(3.88 \times 10^1 \text{ m/s})$ then it begins to decrease gradually until it stabilizes. At the lowest temperature point, $(2.68 \times 10^1 \text{m/s})$ starting from the top of the trombe wall to the rest of the room.

III.5.3 Bottom outlet

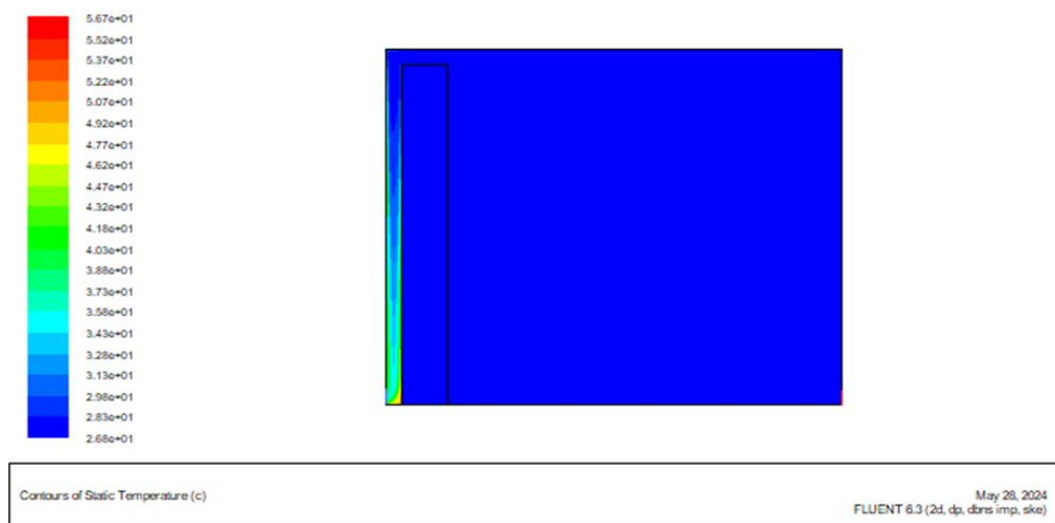


Figure III-10: Contours of static temperate (C°) [Bottom Outlet0.01]

The (Figure III-11) represents the changes of air speed in a room equipped with a trombe wall with dimensions of $(4 \text{ m} \times 3 \text{ m})$ in the case of the air outlet at the bottom, where we notice that the air speed is average at the entry opening at the bottom of the trombe wall at a speed of $(1.97 \times 10^{-1} \text{m/s})$ and begins to decrease as we rise with the trombe wall in values ranging between $(1.85 \times 10^{-1} \text{ m/s})$ to $(1.73 \times 10^{-1} \text{m/s})$ then it reaches a maximum value at the upper opening of trombe's wall at $(2.22 \times 10^{-1} \text{m/s})$ then it returns and rises as we get closer to the exit opening at the bottom of the wall, at values ranging between $(8.63 \times 10^{-2} \text{m/s})$ $(1.73 \times 10^{-1} \text{ m/s})$.

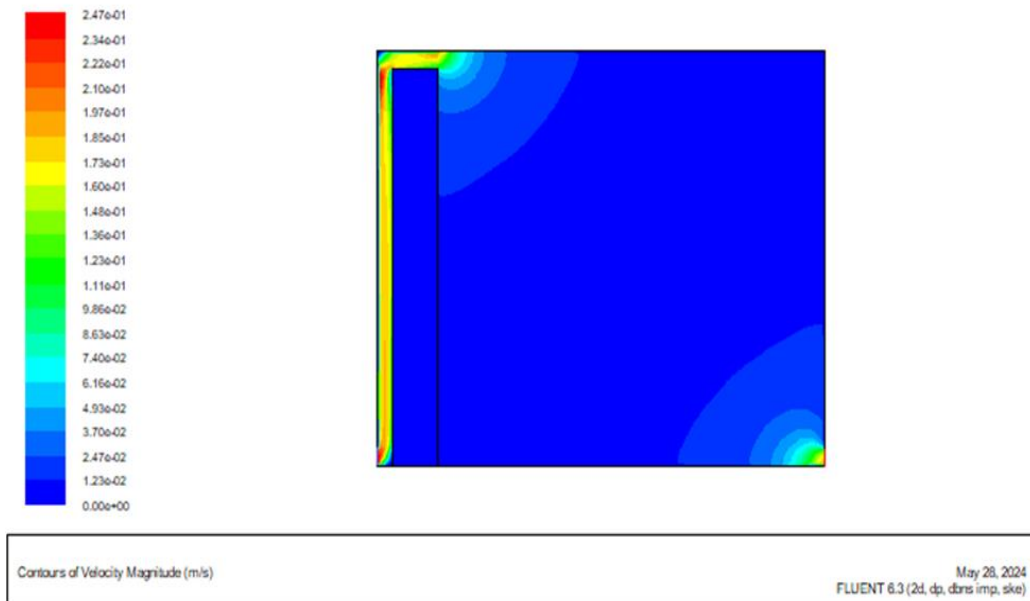


Figure III-11: Contours of static Velocity (m/s) [Bottom Outlet 0.01].

The curve in (Figure III-12) represents the changes in air speed in a living room equipped with a trendy area with a lower outlet opening. we notice that the air speed started from a large value at $(2.00 \times 10^{-1} \text{ m/s})$ and begins to decrease gradually until it reaches a minimum value of (1.20×10^{-1}) then we notice from the curve that air transmission stops for a period. then it returns to zero m/s.

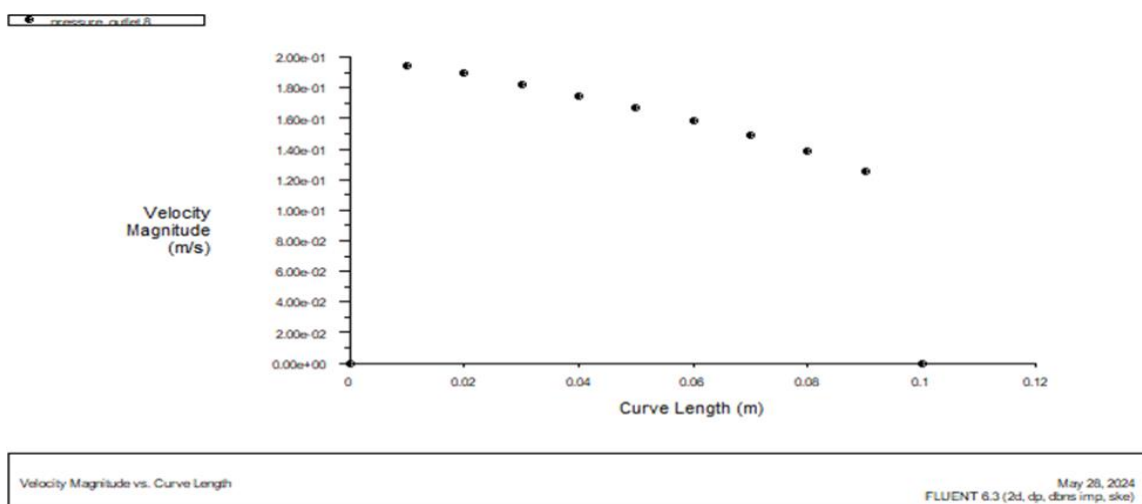


Figure III-12: Velocity change curve as a function of distance.

- From analyzing the previous results, we find that the opening at the bottom of the wall was the most effective in distributing heat within the living room, compared to the upper and middle openings, and the lower air velocity in case of air outlet at the bottom of the wall about $(1.20 \times 10^{-1} \text{ m/s})$.

III.6 Conclusion

The study summarizes that the principle of passive solar heating systems is to use solar energy to heat buildings without the help of technology. The trombe wall system can be an effective passive solar system from the point of view of energy saving, indoor temperature comfort and sustainability assuming proper configuration with an inlet hole for outside air. The position of the hole for the air outlet is changed in the right wall, the first at the top of the wall, the second at the middle and the last at the bottom of the wall. Most solar energy is obtained through glass. The results of the two-dimensional analysis showed that hot air enters the living space and gives a heating effect with the highest temperature and velocity when the opening is at the bottom of the wall.

General Conclusion

General Conclusion

The application of natural ventilation and passive heating, methods is the greatest solution for providing thermal comfort while saving energy, considering the diverse range of types available, the selection should align with the climate of the studied area to optimize the utilization of all the variables.

The study area in the city of Ouargla is considered a desert climate, which makes it ideal for solar thermal energy applications, it is characterized by the largest number of sunny days throughout the year. an example of thermal applications, the subject of our study, is the trombe wall which is considered suitable for the climate of the region .

The main objective of this research is to work on studying the effect of trombe wall in retaining heat inside a living room with proper ventilation was examined, and the results of two-dimensional numerical simulations carried out using gambit and fluent programs were compared.

In our work, we used a design for a living room with certain dimensions that includes a trombe wall with changing the levels of the outlet opening in the opposite wall at the top, middle and bottom of the wall, from the simulation outputs and numerical results, we find that the opening at the bottom of the wall opposite the trombe wall can contribute to increasing heating efficiency ,this is because it allows the cold air that collects at the floor to move outward and allows the hot air to descend from above.

Choosing the trombe wall method for heating is considered the ideal option because it is able to use energy effectively as it can save space in the room to be heated, and it is the ideal solution in areas isolated from electricity and gas stations. finally, it provides greater safety compared to home heating devices that use electricity and gas as there is no Potential risk of harmful emissions or human safety.

Abstract

This research presents the effectiveness of a trombe wall on the heating of a living room using the Gambit design and fluent program. 2D computational fluid dynamic used to simulate the air velocity and temperature change in a room with dimensions (3 m × 4 m). In order to find the best grid size, a different size has been proposed 0.05, 0.01, 0.005, and 0.1 and compared. The proposed system have a three different configurations; Configuration I contains a simple room with a Trombe wall and the outlet opening located in the top wall. Configuration II contains a simple room with a Trombe wall and the outlet opening located in the bottom wall. Configuration III contains a simple room with a Trombe wall and the outlet opening located in the middle wall. The grid size test results show that (0.01) is most suitable for a best heat and velocity distribution. Moreover, it can be seen clearly that at the top, the air speed was fast and the efficiency of heat distribution was lower. The second level was in the middle at a lower speed than the first, and the third level was the opening at the bottom of the wall with better efficiency in heat distribution and the air ventilation speed was lower. The simulation results helped us to study the effect of the Trombe wall on heat retention and increasing heating inside the room with appropriate air outlet for more efficient heat diffusion. The minimum air velocity at the chamber outlet was found to be $(1.92 \times 10^{-1} \text{ m/s})$ at the bottom.

Keywords: Trombe wall , heating , air velocity , simulation .

Résumé

Cette recherche présente l'efficacité d'un mur Trombe sur le chauffage d'un salon en utilisant la conception Gambit et le programme fluent. Dynamique des fluides informatique 2D utilisée pour simuler la vitesse de l'air et le changement de température dans une pièce de dimensions (3 m × 4 m). Afin de trouver la meilleure taille de grille, une taille différente a été proposée 0,05, 0,01, 0,005 et 0,1 et comparée. Le système proposé a trois configurations différentes ; La configuration I contient une pièce simple avec un mur Trombe et l'ouverture de sortie située dans le mur supérieur. La configuration II contient une pièce simple avec un mur Trombe et l'ouverture de sortie située dans le mur inférieur. La configuration III contient une pièce simple avec un mur Trombe et l'ouverture de sortie située dans le mur du milieu. Les résultats des tests de taille de grille montrent que (0,01) est le plus approprié pour une meilleure répartition de la chaleur et de la vitesse. De plus, on voit clairement qu'au sommet, la vitesse de l'air était rapide et l'efficacité de la distribution de la chaleur était moindre. Le deuxième niveau était au milieu à une vitesse inférieure à celle du premier, et le troisième niveau était l'ouverture au bas du mur avec une meilleure efficacité dans la distribution de la chaleur et la

vitesse de ventilation de l'air était plus faible. Les résultats de la simulation nous ont aidé à étudier l'effet du mur Trombe sur la rétention de chaleur et l'augmentation du chauffage à l'intérieur de la pièce avec une sortie d'air appropriée pour une diffusion plus efficace de la chaleur. La vitesse minimale de l'air à la sortie de la chambre s'est avérée être de $(1,92 \times 10^1$ m/s) au fond.

Mots clé : Mur Trombe, chauffage, la vitesse de ventilation, simulation .

ملخص

يعرض هذا البحث فعالية جدار ترومب على تدفئة غرفة المعيشة باستخدام تصميم وبرنامج Fluent . Gambit ديناميكية الموائع الحسابية ثنائية الأبعاد تستخدم لمحاكاة سرعة الهواء وتغير درجة الحرارة في غرفة ذات أبعاد $(3 \times 4$ م). من أجل العثور على أفضل حجم للشبكة، تم اقتراح حجم مختلف 0.05 ، 0.01 ، 0.005 ، و 0.1 ومقارنتها. يحتوي النظام المقترح على ثلاثة تكوينات مختلفة؛ يحتوي التكوين الأول على غرفة بسيطة بجدار ترومب وفتحة المخرج الموجودة في الجدار العلوي. يحتوي التكوين الثاني على غرفة بسيطة بجدار ترومب وفتحة المخرج الموجودة في الجدار السفلي. يحتوي التكوين الثالث على غرفة بسيطة بجدار ترومب وفتحة المخرج الموجودة في الجدار الأوسط. أظهرت نتائج اختبار حجم الشبكة أن (0.01) هو الأكثر ملاءمة لتوزيع أفضل للحرارة والسرعة. علاوة على ذلك، يمكن أن نرى بوضوح أنه في الأعلى، كانت سرعة الهواء سريعة وكفاءة توزيع الحرارة أقل. المستوى الثاني كان في المنتصف بسرعة أقل من الأول، والمستوى الثالث كان عبارة عن فتحة في أسفل الجدار بكفاءة أفضل في توزيع الحرارة وسرعة تهوية الهواء أقل. ساعدتنا نتائج المحاكاة في دراسة تأثير جدار ترومب على احتباس الحرارة وزيادة التدفئة داخل الغرفة مع وجود مخرج هواء مناسب لانتشار الحرارة بشكل أكثر كفاءة. وجد أن أقل سرعة للهواء عند مخرج الغرفة هي $(1.92 \times 10^1$ م/ث) في الأسفل.

الكلمات المفتاحية : جدار ترومب، تسخين، سرعة الهواء، المحاكات .

Bibliography

- [1]-Omar Ellabbana / HaithamAbu-Rubb /Frede Blaabjergc, Renewable energy resources: Current status, future prospects and their enabling technology.
- [2]- M. Iman Abdel Hadi Al-saaida, (2-03-2022) Heating, Ventilation and conditioning HVAC system Arab journal for scientific publishing , ISSN:2663-5798 p41.
- [3]- Nabil Farag Al-Hassan. Passive use of solar energy to heat buildings. Higher Institute of Professions, Misrata, Libya 2014
- [4]- Danijela Nikolić / Jasmina Skerlić / Dragan Cvetković / Jasna Radulović / Saša Jovanović BASIC PRINCIPLES OF PASSIVE SOLAR HEATING. Center for Quality, Faculty of Engineering, University of Kragujevac . Serbia Novembre2018.
- [5]- Omidreza Saadatiann , K.Sopian,C.H.Lim , Nilofar Asim , M.Y.Sulaiman , Trombe walls: Review of opportunities and challenges in research and development, Université Kebangsaan Malaysia ,43600Bangi,Selangor,Malaysia.
- [6]- Abraham Yezioro, A knowledge based CAAD system for passive solar architecture, Faculty of Architecture and Town Planning, Technion-Israel Institute of Technology ,Haifa 32000.
- [7]- SARMOUK Mohammed Dhiya-Eddie, Experimental and numerical development of a hybrid solar/gas heating system ,PhD thesis. École Nationale Polytechnique, 2021.
- [8]- Ruchi Shukla ,K . Sumathy ,Phillip Erickson, Jiawei Gong, Recent advances in the solar water heating systems : A review, Department of Mechanical Engineering ,North Dakota State University ,PO Box 60 50 ,Fargo ,ND58108, USA.
- [9]- Heba Mahmoud Fouad, Ayman H. Mahmoud & Rania Rushdy Moussa, Effect of a geothermal heat pump system on cooling residential buildings in a hot dry climate, HBRC Journal, 19:1, 483-507, DOI: 10.1080/16874048.2285095, 2023
- [10]- Soltani, F.M. Kashkooli, A.R. Dehghani-Sanij, A.R. Kazemi, N. Bordbar, M.J. Farshchi, M. Elmi, K. Gharali, M.B. Dusseault, A comprehensive study of geothermal heating and cooling systems,28-9-2018.
- [11]-Justen Forrest, Geothermal Heat Pumps, Blue Horizons Project, BHP Education Articles,2020.

[12]- Sabrin Korich. Etude du gisement géothermique et exploitation de la géothermie pour les diverses applications dans les régions arides et semi-arides Study of the geothermal field and the exploitation of geothermal energy for the various applications in arid and semi-arid region ,University of Ouargla Algeria 17/02/2021.

[13]- Dridi Yacine Ben dada Med Lazhar ,Estimation du potentiel Biomasse en Algérie ,Université kasdi merbah Ouargla faculté des sciences appliquées 07/06/2015.

[14]- Dridi Yacine Ben dada Med Lazhar/ poster: (Estimation du potentiel Biomasse en Algérie) Université kasdi merbah Ouargla faculté des sciences appliquées 12/05/2015.

[15]-Shiva Kumar/ Hankwon Lim, An overview of water electrolysis technologies for green hydrogen Production, 21/07/2022.

[16]- Sofiane Bahria , Madjid Amirat , Abdelrahman Hamidat , Mohammed El Ganaoui , Mohamed El Amine Slimani, Parametric study of solar heating and cooling systems in different climates of Algeria e A comparison between conventional and high-energy-performance buildings, Université des Sciences et de la Technologie Houari Boumediene, BP 32 El Alia, Bab-Ezzouar, Algiers, Algeria.

[17]- Adnane Labeled , Amar Rouag , Adel Benchabane , Nouredine Moumami , Mohammed Zerouali

Applicability of solar desiccant cooling systems in Algerian Sahara: Experimental investigation of flat plate collectors, 1-Laboratoire de Génie Mécanique (LGM), Université de Biskra, B.P. 145 R.P. 07000, Biskra, Algeria

2 -Laboratoire de Génie Energétique et Matériaux (LGEM), Université de Biskra, B.P. 145 R.P. 07000, Biskra, Algeria

- [18]- Abdelazim Abbas Ahmed 1,* , Mohsen Assadi 1 , Adib Kalantar 2 , Tomasz Sliwa 3 and Aneta Sapińska-Sliwa 3. A Critical Review on the Use of Shallow Geothermal Energy Systems for Heating and Cooling Purposes, Review on the Use of Shallow Geothermal Energy Systems for Heating and Cooling Purposes, *Energies* 2022, 15, 4281. <https://doi.org/10.3390/en15124281>
- [19]- D. Romanov , B. Leissa, Geothermal energy at different depths for district heating and cooling of existing and future building stock, *Renewable and Sustainable Energy Reviews* 167 (2022) 112727, e 25 June 2022.
- [20]- Kaushikk Ravender Iyer, Hamid Roozbahani , Marjan Alizadeh, Heikki Handroos, A novel approach for direct conversion of wind energy to heat utilizing a hydraulic medium for domestic heating applications, *Energy Reports journal*, 8 .11139–11150, (2022).
- [21]- Amir mohamed Behzadi a,* , Sasan Sadri Zadeh a,b A rule-based energy management strategy for a low-temperature solar/ wind-driven heating system optimized by the machine learning-assisted grey wolf approach, *Energy Conversion and Management* 277. 116590,2023
- [22]- GUERROUT Abdessamad et BOUDINA Youcef ;Mémoire MASTER ; Étude Expérimentale Et Simulation Numérique De La Ventilation Naturelle Dans Un Bâtiment Associé A Une Cheminée Solaire Et Une Tour A Vent Dans Un Climat Semi-Aride 13/06/2022
- [23]-Mohammed ZELACI Riad HERR ; Mémoire MASTER ACADEMIQUE Optimisation et simulation numérique d'un nouveau de refroidissement par un échangeur de chaleur air sol couplée avec une tour du vent sous un climat aride 14/06/2022
- [24]- Wang.L at al , A CFD Simulation of 3D Air Flow and Temperature Variation in Refrigeration Cabinet, The 7th World Congress on Particle Technology (WCPT7), China, 2015.
- [25]-Dr. G.S.V.L Narasimham , A PASSIVE SOLAR WINTER HEATING SYSTEM BASED ON, *INTERNATIONAL JOURNAL OF INNOVATIONS IN ENGINEERING RESEARCH AND TECHNOLOGY* , India 2016
- [26]- Mr. MAHMA Hassen Mr. BERGHOUTI Farouk, La filière avicole (poulet de chair) dans la wilaya de Ouargla : autopsie de dysfonctionnement Cas de la région de Ouargla 2015/2016.
- [27]- Moufida Sebtia, Djamel Alkamaa , Ammar Bouchareb. Assessment of the effect of modern transformation on the traditional settlement 'Ksar' of Ouargla in southern Algeria. Biskra, University Mohamed Khider, 16 May 2013.
- [28]- <https://www.tutiempo.net/amp-fr/climat/01-2023/ws-605800.html>

[29]- Mouna Abarkan / M'Sidi Nacer Kouider, Modélisation et Analyse du comportement d'un Bâtiment équipé d'un Système Multi Sources d'énergie, l'université sidi mohamed Ben Abdellah. 9/12/2014.

[30]- Dr. G.S.V.L. Narasimham / Prof. K.S.Ravi / Abhilash A.N, STUDY OF A PASSIVE SOLAR WINTER HEATING SYSTEM BASED ON TROMBE WALL.